7. GEOMECHANICAL DESIGN AND PERFORMANCE ASSESSEMENT–PRECLOSURE GROUND SUPPORT AND POSTCLOSURE DRIFT DEGRADATION ANALYSES

As the rock mass material models and property ranges are defined, numerical models can be used for design and sensitivity studies to examine two major issues addressed in the RDTME KTI agreements. The first issue is the postclosure drift degradation resulting from thermally induced stresses, seismically induced rockfall, and possible static fatigue mechanisms. The second is the preclosure ground support design and evaluation as well as an inspection and maintenance strategy. Each of these issues is discussed here.

7.1 ANALYSIS OF ROCKFALL UNDER POSTCLOSURE SEISMIC SHAKING

The potential exists for rockfall to occur as a result of shaking induced by earthquakes. The current emplacement drift concept calls for waste packages to be placed on a metal pallet structure that will rest on an engineered, compacted fill in the invert of the 5.5 m diameter emplacement drifts. At postclosure, current design calls for the waste package to be covered with a continuous "drip shield" constructed of titanium that will act as both a seepage cover and a rockfall shield.

7.1.1 General Methodology

It is the intent of the rockfall analyses to quantify possible seismically induced rockfall (and, ultimately, drip shield and waste package mechanical damage) over the 10,000 year regulatory postclosure period. A general methodology for conducting these studies is given in Figure 31. Geologic mapping will be used to define a "synthetic" or representative rock mass that can be sampled randomly to create possible rock masses in which the tunnel can be simulated. Numerical models (two- or three-dimensional, depending on the lithology in question), with input geometry and properties based on the geologic variability, will be used to make rockfall estimates for seismic events whose magnitude is based on the probability of occurrence in terms of annual exceedance frequency. For each annual exceedance frequency, a number of probabilistically determined, site-specific ground motions will be developed and used to provide the transient boundary conditions to the models. The resulting rockfall, in terms of the tonnage of the maximum size rock particle, total tonnage for a given simulated length of tunnel, and the velocity of rock particles, will be determined. A number of simulations will be conducted for each annual exceedance probability in which the rock mass geology and site-specific ground motion will be randomly sampled. The ultimate goal will be to conduct sufficient simulations to produce a probability density function of rockfall as a function of peak ground velocity level such that a mean and standard deviation can be defined. The rockfall is then used as input to the structural analysis of impact loading on the drip shield.

7.1.2 Site-Specific Ground Motions

Site-specific ground motions will be determined based on the estimates of peak ground acceleration or peak ground velocity obtained from the seismological expert elicitation process conducted previously (CRWMS M&O 1998a). The probabilistic seismic hazard assessment process resulted in an estimate of the earthquake source characteristics and source locations as a

function of their probability of occurrence, expressed in terms of peak ground acceleration or peak ground velocity for a given annual exceedance probability (probability of occurrence per year). The resulting relationship of annual probability and peak ground velocity is termed the hazard curve.

For each annual hazard level, a number of ground motions (15 are currently anticipated) representing characteristics from distinct actual earthquakes are compiled with magnitude, focal distances and frequency characteristics consistent with *Probabilistic Seismic Hazard Analyses for Fault Displacement and Vibratory Ground Motion at Yucca Mountain, Nevada* (CRWMS M&O 1998a). The ground motions are selected to represent the variability of the potential ground motions. Each ground motion consists of three time history components: one vertical and two horizontal. These ground motions are scaled to the peak ground velocity for a given annual exceedance frequency derived from the hazard curve.

7.1.3 Numerical Modeling Approach

As discussed in depth earlier, it is anticipated that the lithophysal and nonlithophysal rock masses will respond in distinctly different fashion from the seismic shaking. The modeling assumptions and methods to be used for each of these rock types are discussed below.

7.1.3.1 Nonlithophysal Rocks

Due to the high intact strength and fracture-controlled nature of the nonlithophysal rocks, the following preliminary conclusions can be drawn:

1. The problem is three-dimensional and anisotropic in nature.

2. Failure and rockfall response is a function of fracture orientation, continuity, the resulting block geometry, fracture properties and ground motion characteristics.

As a result of the above, the 3DEC program is used for modeling of nonlithophysal rocks. This program is fully dynamic in nature, with provision for applying transient boundary conditions, and allows non-reflecting and free-field dynamic boundaries. The rock mass is represented as a number of intact rock blocks that are separated by interface planes whose mechanical behavior are represented by a standard Mohr-Coulomb slip condition. The intact blocks are subdivided into tetrahedral finite difference zones, and can be assigned any desired mechanical constitutive law. Here, due to the high strength of the rock mass, it is assumed that the blocks behave elastically.

The most important aspect of the 3DEC modeling is implementing the field fracture geometric data into the model, followed by the subsequent formation of blocks. This is particularly important since the fractures within the Tptpmn are non-persistent in nature, with mean trace lengths smaller than the diameter of the tunnel (i.e., many of the fractures are of insufficient length to form a regular block geometry). The fracture geometries used as input to 3DEC are derived from the FracMAN simulations as discussed in Section 6.1.2. Modifications to the 3DEC program have been made to accommodate the FracMAN output; namely, the discontinuous nature of the fractures. Previously, 3DEC had assumed that fractures are continuous in nature, and thus it was impossible to have a fracture that ends in solid rock. The

program now allows circular or rectangular fracture surfaces consistent with FracMAN by bonding all fracture contact points outside the defined fracture surface. In this manner, it is possible for the contacts to be given the equivalent properties of the solid rock, thus joining the adjacent blocks to form a discontinuous fracture.

The detailed modeling methodology is illustrated in Figure 32. A number of potential fracture geometries (approximately 100 for each hazard level) are selected by generating random tunnel centroid locations within a 100 m cube of simulated FracMAN rock mass. At each of these locations, a representative rock mass volume, approximately two tunnel diameters around the tunnel centroid and 25 m in length, is selected. This volume is considered sufficient to contain the limits of damaged rock, and of sufficient length (approximately 5 times the tunnel diameter and over 10 times the mean trace lengths) to provide a representative volume for rockfall. For each of these volumes, a simulated full-periphery map can be developed to verify, from a practical geological perspective, that the fracture geometries are realistic. The outer boundaries of the 3DEC model are much larger than this internal, fractured zone, such that boundary effects are minimized.

One of the approximately 15 ground motions and one of the 100 fracture geometries are then randomly selected for each dynamic analysis. A base case of rock and fracture properties will be defined from existing data and used for the initial set of runs. This base case will use the best estimate intact elastic properties as well as the joint cohesion, stiffness and friction properties. Conservative assumptions will be made such that the joints are smooth and planar (i.e., zero dilation). The gravitational and mining-induced stresses will be defined as the initial state prior to seismic load application. The general factor of safety of the block system under gravitational load will be defined as the starting condition, followed by application of the ground motion.
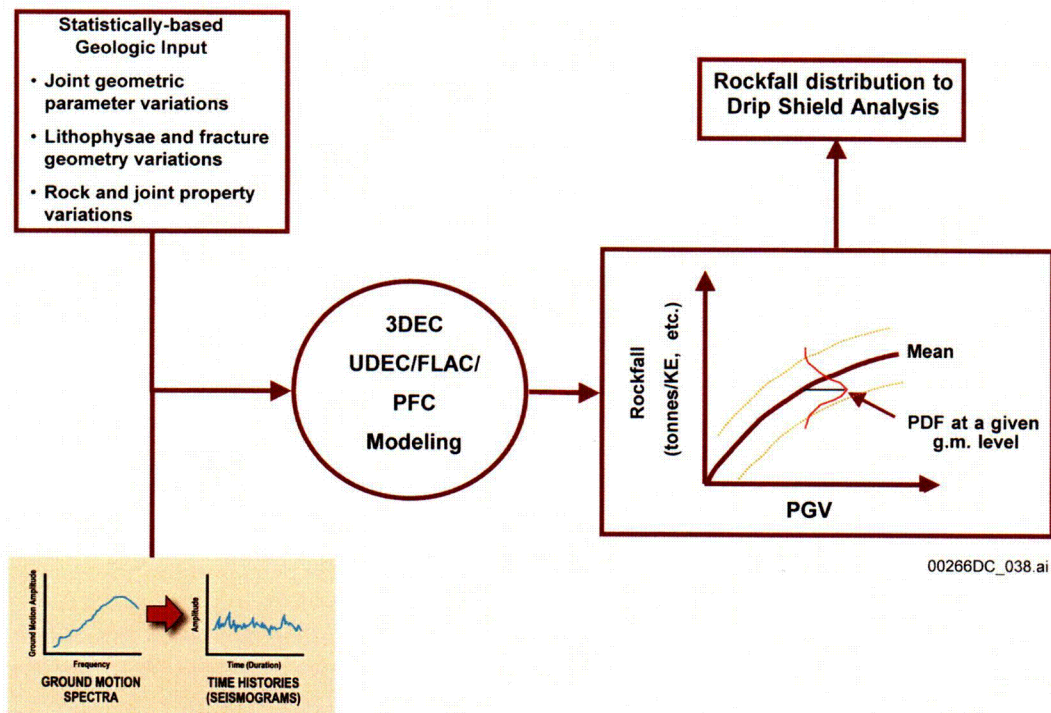

Figure 31. General Procedure for Rockfall Analysis

The total number of runs to be made (probably greater than 50) is unknown at present, and can only be determined once the rockfall statistics are compiled and its variability determined. The output of the runs, as mentioned earlier, will be in terms of the mass and velocity of each block that is ejected and strikes the drip shield as well as the total mass of blocks. The location of each impact will be defined for ease of input to the structural analysis of the drip shield. After these initial runs are completed, which examine the variability of rockfall as a function of fracture geometry and ground motion, a series of simulations with selected models that span the range of greatest to least rockfall, will be run to examine the impact of the following items:

- Fracture properties–friction angle, dilation angle, cohesion, and fracture stiffness.

- Thermally induced stresses–thermal stresses derived from the regional topographic analysis described earlier will be applied as initial conditions. A number of points in time such as the peak stress condition and the equilibrium state after cool-down will be used.

The results of these runs will be compared to the compiled base case statistics to identify the impact of environment or properties variations on rockfall.

7.1.3.2 Lithophysal Rocks

Modeling Assumptions
The basic assumptions regarding lithophysal rocks include:

- Mechanical constitutive response is controlled by lithophysal porosity and inter-lithophysal fracture density. Constitutive behavior is determined by calibrating discontinuum model to lab and in situ testing data.

- Rock mass can be considered isotropic and homogeneous.

- Block size distribution a function of inter-lithophysal fracture density and lithophysae spacing.

- Amount of rockfall can be estimated from sensitivity analyses using bounding properties based on laboratory and in situ testing results.

- Two-dimensional modeling is adequate.

Modeling Methodology
The methodology proposed to perform the rockfall estimates within the lithophysal units is given in Figure 33. This flow diagram indicates that the UDEC program will be the primary modeling tool used to conduct parametric analyses of the range of assumed lithophysal rock properties derived from the large core testing of the Tptpul and Tptpll. As shown, the size of rock particles that are created from the lithophysal rocks will be estimated from geologic and empirical evidence and will not be calculated from the numerical modeling. As described previously, the Tptpll has a ubiquitous, short length interlithophysal fracturing fabric with spacing on the order of 1 to 2 in., while the large trace length, natural joints are widely spaced and discontinuous. The

ubiquitous fractures, combined with the relatively abundant uniformly spaced lithophysae (that also provide natural breaking surfaces), the result is block sizes on failure that are on the order of a few inches in diameter. There is significant observational information in the tunnel that supports this assumption. For example, rock yield along the ribs of the ECRB indicates the rock tends to break into very small block sizes when stressed. Large-core drilling in the ECRB for the purpose of obtaining test samples shows abundant natural fractures between lithophysae (Figure 34). As seen in this photo, the fractures and lithophysae result in intact blocks that are a few inches across. This natural fracturing has resulted in significant difficulty in obtaining intact core lengths greater than a foot in length.

Calibration of the UDEC Model to Represent an Equivalent Lithophysal Rock Mass
The issue of numerical representation of lithophysal rocks and how this is used in a seismic analysis is documented here. It is numerically too large of a problem for a model such as PFC be used to attempt to represent the lithophysae structure and fractures in a tunnel-scale model. A method needs to be devised to represent a "mechanical equivalent" lithophysal material that incorporates the lessons learned from the testing and PFC modeling into a simpler numerical tool. Typically, a continuum constitutive model based on some form of shear and perhaps void compaction yield surfaces would be derived from the laboratory and in situ test data. This model would be embedded within a suitable dynamic numerical approach and used to estimate the failure mode and extent resulting from the earthquake excitation. The problem with a continuum-based approach is that it does not allow estimation of how much rock actually detaches itself from the rock mass, and bulks in the excavation. To overcome this problem, we propose here to calibrate a mechanically equivalent discontinuum model within the UDEC program. This model will provide the lithophysal rock mass yield behavior, but will also allow the rock mass to break into small blocks under the action of the dynamic stresses. The process of calibration of the model is described in detail below.

UDEC is a two-dimensional large-displacement discontinuum program. To determine the overall damage zone around the tunnels and the portion of that zone that is expected to dislodge and fall, the rock mass is subdivided into many small, irregularly shaped blocks that are much smaller in dimension than the tunnel diameter (Figure 35). The contacting surfaces between blocks have normal and shear stiffnesses that are matched to the elastic properties of the blocks themselves, thus creating a mass with isotropic elastic behavior. The contacting surfaces are also bonded with a shear and tensile strength to provide the overall rock mass shear and tensile failure characteristics. The overall behavior of this system—its elasticity and failure characteristics—is calibrated to laboratory and in situ testing.

Thus, this approach is similar to development of a continuum-based mechanical constitutive law with one important difference–the discontinuum method provides for discrete fracture or failure networks to develop when stressed, thereby providing realistic failure mechanisms and the ability to form detached blocks. The detached blocks may consist of one or more of the basic unit blocks within the model. Of course, the primary limitation of this method is the block size needs to be smaller than the expected size of the detached blocks. The size of the unit blocks that make up the model will be verified during calibration and testing.
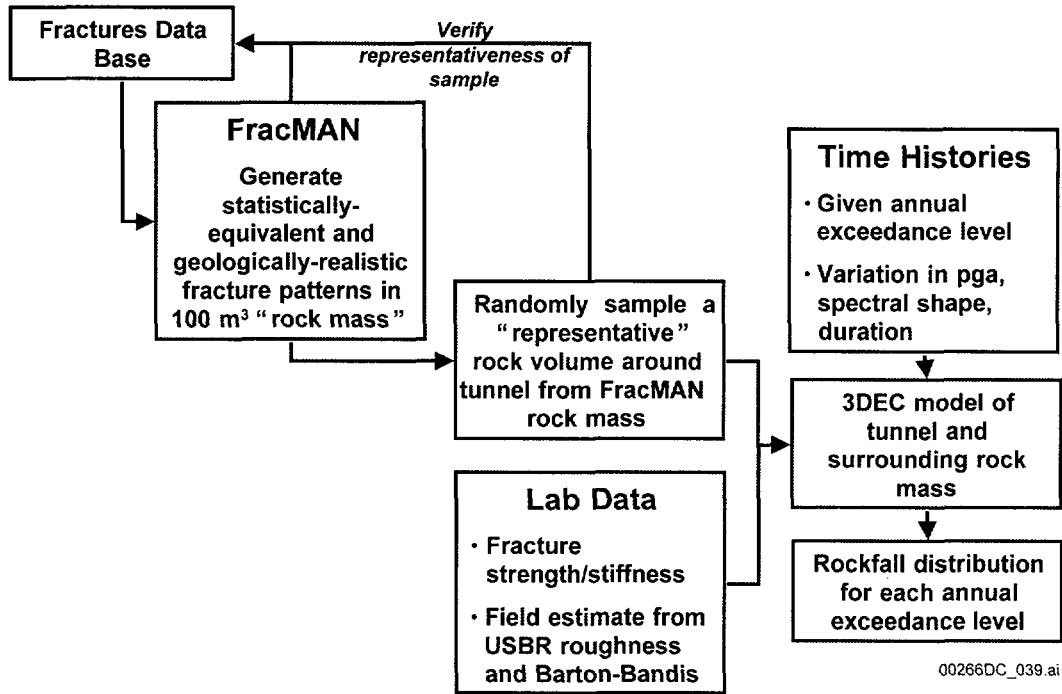
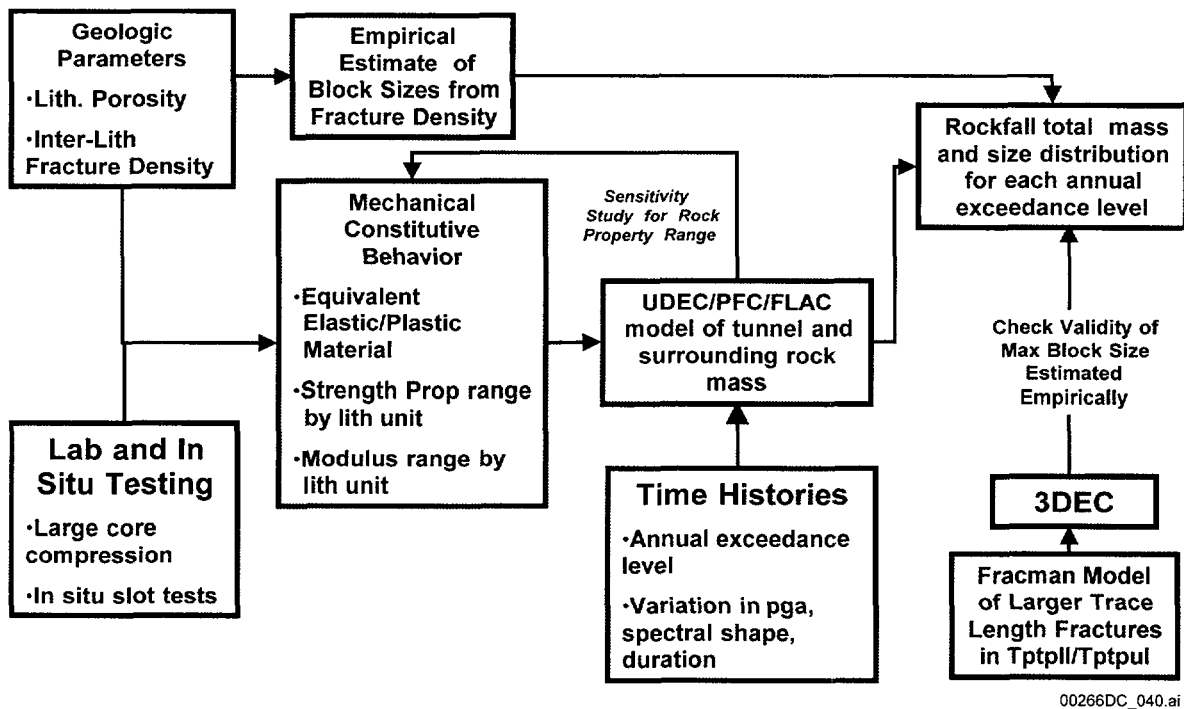Figure 32. General Methodology for Rockfall Calculations in the Nonlithophysal Rocks

Figure 33. Methodology for Rockfall Analysis in Lithophysal Rocks

00266DC_041.ai

NOTE: A core sample from the Tptpll with a diameter of 12 in. (30.5 cm). Note the widespread, closely spaced fracturing along the length of the sample. The core will fail along these preexisting fractures.

Figure 34. Example of a Core Sample from the Tptpll

Laboratory and field testing is currently underway primarily on lithophysal rocks to supplement the existing database. The existing core testing from the Tptpul and Tptpll described earlier, showing a uniaxial compressive strength range from approximately 10 to 30 MPa and Young's Modulus of about 10 to 23 GPa will be used initially for calibration of the range of properties for the UDEC model. The equivalent UDEC model rock mass will be calibrated against the laboratory compression test data to ensure that the correspondence of the model to rock behavior is understood. In many ways, this calibration process is similar to that described for the PFC program earlier. The calibration is run by conducting numerical tests on "core" samples that have been "extracted" from the UDEC tunnel model block structure, much as one would take a rock core from the field and test in the laboratory. This rock sample is then tested in uniaxial and triaxial compression, and the output stress-strain response determined. The block surface contact properties are adjusted to achieve a calibration against the lab and in situ testing. Figure 36 shows an example of such a calibration of model stress-strain response and failure mechanism for the case of a higher strength lithophysal rock with a UCS of 20 MPa. The figure shows the ability of the model to produce typical failure modes that are observed in the lab testing–from axial splitting in uniaxial compression to shear failure modes in confined compression. Many parameter analyses with varying block sizes and shapes as well as surface properties will allow a detailed understanding of the actual material behavior that is represented by the model. In other words, numerical experiments will be performed so that the material response that is modeled is fully transparent. Since it is very difficult to conduct true triaxial compression tests on large lithophysal core, it is planned to use the calibrated PFC model to numerically examine the mechanical effects of confinement on lithophysal rocks. The PFC model is currently being calibrated against the UCS testing to achieve an understanding of the impact of porosity on both modulus and strength. The PFC model will then be used to conduct triaxial tests on three-dimensional "samples" of various porosity to understand the postfailure dilation properties of the material, thus allowing development of a true shear and compaction constitutive model for

C02

the lithophysal rock. These results will be used to verify that the UDEC model reasonably represents postpeak response (dilation) for varying levels of porosity.
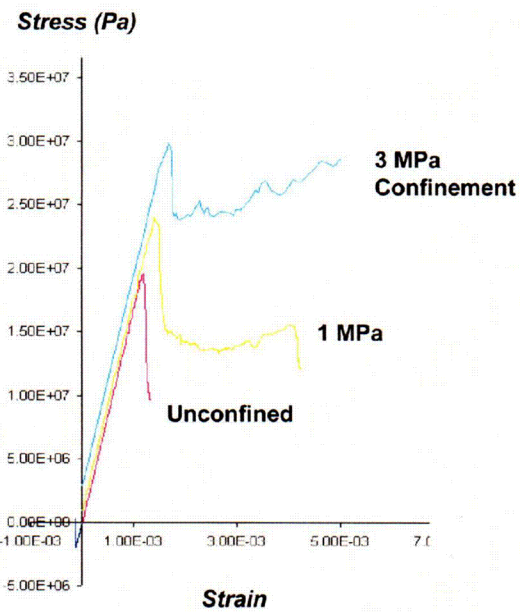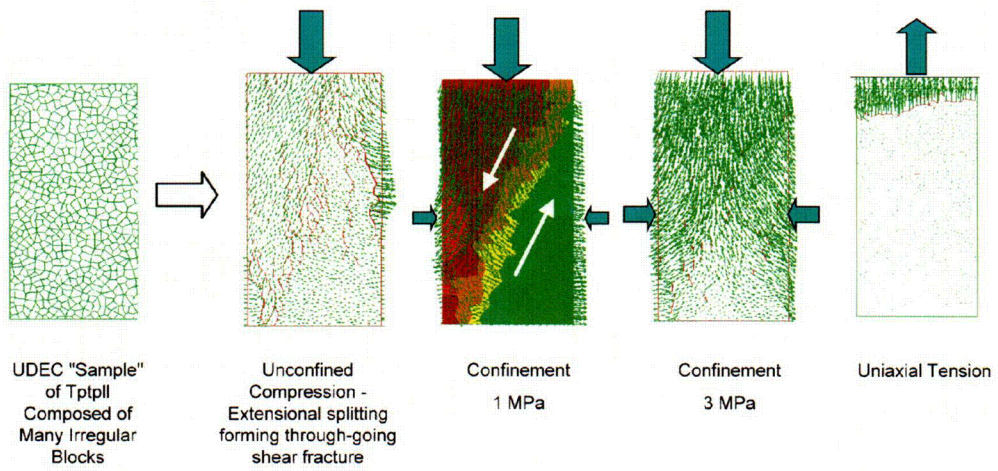
Rockfall Parametric Analyses
It is the intent to calibrate a number of UDEC representations of lithophysal rock with varying levels of porosity that span the range from lowest to highest strength and deformability. For each ground motion annual exceedance level, a parametric study will be conducted in which the strength and deformability properties of the UDEC model will be varied from lowest to highest strength in approximately 5 steps. These 5 property cases will be randomly matched to one of the approximately 15 ground motions to examine effects of both properties and ground motion variability. The total number of analyses will be determined empirically, as the variability in the response becomes evident.

00266DC_042.ai
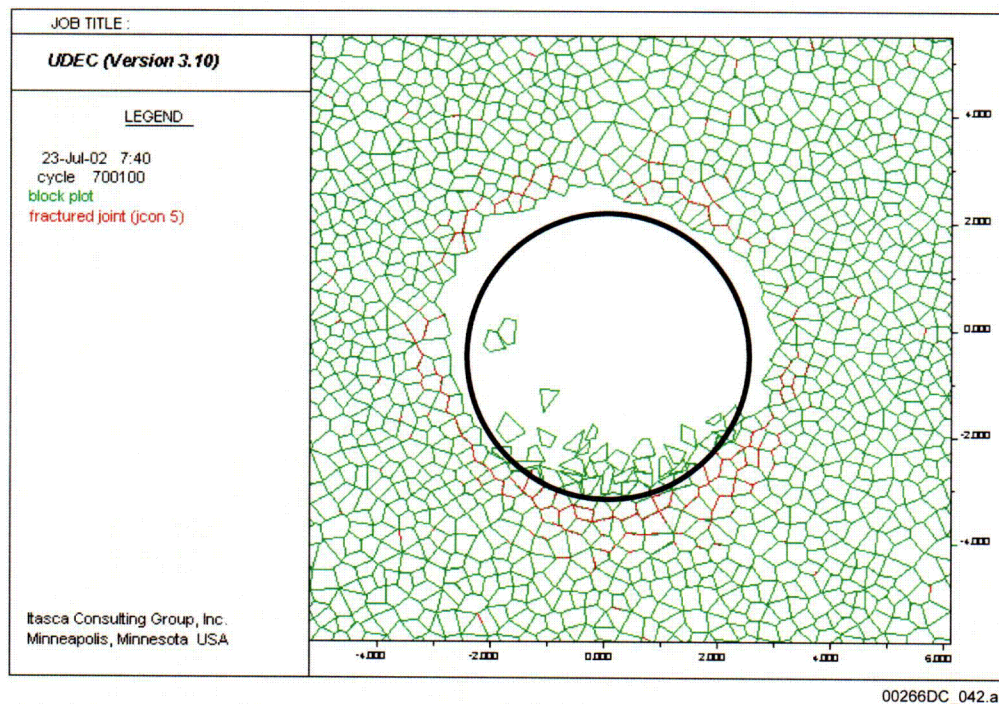
NOTE: This figure shows subdivision of the rock mass into many small and irregular blocks whose equivalent behavior conforms to an elastic-plastic material with Mohr-Coulomb yield condition. Seismic shaking results in blocks breaking free from the rock mass falling into the tunnel. Developing shear or extensional fractures are shown in red. Units are in meters.

Figure 35. Conceptual UDEC Model of Lithophysal Rocks

UDEC "Sample" of Tptpll Composed of Many Irregular Blocks

Unconfined Compression - Extensional splitting forming through-going shear fracture

Confinement 1 MPa

Confinement 3 MPa

Uniaxial Tension

Stress (Pa)

3 MPa Confinement

1 MPa

Unconfined

Strain

00266DC_043.ai

NOTE: This approach shows uniaxial and triaxial compression testing. Spontaneous sample failure modes occur as the sample is compressed, and the resulting equivalent rock mass stress-strain curves are shown here. The unconfined strength and modulus is calibrated to measured laboratory behavior.

Figure 36. Example of UDEC model Calibration Approach

c04

7.2 THERMAL LOADING EFFECTS AND LONG-TERM STRENGTH DEGRADATION

7.2.1 Discussion

The rock mass surrounding the excavations may undergo damage from thermally induced stresses and/or time-dependent damage associated with static fatigue resulting from stress corrosion mechanisms. This damaged material may result in a slow unraveling (Tptpll) or block fallout (Tptpmn) mode of failure with some extent of drift filling. The effect of thermal stress on rock failure extent can be examined using the numerical techniques discussed in the previous section. Time-dependent degradation—rockfall from a tunnel or other unsupported excavation over long time periods—is currently not well understood, particularly in hard, strong rocks. It certainly seems reasonable that time-related rockfall would be a greater issue in the more heavily fractured rocks such as the Tptpll, and will be related to the ratio of induced stress to rock mass strength. The goal here is to provide a reasonable estimate of the propensity for yield and rockfall as a function of the induced stress levels and time.

Assume that, over time, the yielded rock surrounding the tunnels (particularly within the Tptpll) begins to ravel and fall as ground support corrodes and loses effectiveness. As fallen rock accumulates on the excavation floor and drip shield, it will increase in volume due to volumetric bulking. Also, the crown of the tunnel would extend vertically in an elliptical fashion. Two mechanisms will eventually arrest the raveling response. First, the confinement at the crown would increase as the excavation becomes more elliptical. Second, the bulking rock volume (which forms a backfill that eventually will choke itself off) will arrest the failure as the confinement supplied by the bulked rock to the excavation walls tends to provide a reinforcing backpressure.

Since the current repository concept involves a drip shield, the fallen rock could eventually build up around the drip shield. It is relevant to examine the time and volume of rock ultimately produced from this degradation process since the settled rock could have impacts on:

- Seismically induced rockfall (non-seismic degradation could reduce or prevent seismically induced rockfall in the lithophysal rocks if it occurs early enough and with enough volume).

- Igneous intrusion mechanisms (it could prevent magma intrusion into tunnels).

- Waste package temperatures and seepage mechanisms.

It would seem reasonable to assume that the mechanism of time-related degradation could be a result of either thermally induced stresses or static fatigue via a stress corrosion mechanism. In the nonlithophysal rocks, static fatigue failure of asperity-related roughness along fracture surfaces is possible, and could result in gravitationally induced block failures through reduction in dilation. Static fatigue of hard rocks typically is associated with stress levels on the order of 80 percent or greater of the uniaxial compressive strength. In the case of the lithophysal rocks, the compressive stress concentrations along the immediate rib springline of the emplacement

drifts is locally near the uniaxial compressive strength at repository depth in the Tptpll, making long-term static fatigue mechanisms of importance.

7.2.2 Approach

7.2.2.1 Thermal Stress Degradation

It is planned to investigate possible thermal stress-induced degradation effects using the same general UDEC model and property ranges described previously for rockfall studies (Section 7.2.3.2). Predicted temperature profiles around emplacement drifts will be predicted using other numerical approaches as part of the waste package and ventilation aspects of the project. The rock mass temperatures from these models for preclosure and postclosure times will be interpolated at gridpoint locations in the UDEC model. These temperatures will then be used to develop the associated thermally induced stresses and produce yield and failure within the fracture network that comprises the equivalent rock mass as described previously. Calculations will be made of the depth of yield, the characteristics of the failing rock mass (i.e., the strains as a function of depth from the tunnel surface), and an estimate of the amount of rock that can potentially detach and fall into the tunnel. These calculations will be done for the range of probable rock mass properties of Tptpll. A validation of the thermal fracturing predictive capability of this approach through back-analysis of the thermally induced roof spalling observed in the Drift Scale Test recently conducted in the ESF. In this test, the room temperature was overdriven (to about 200°C), with resulting minor levels of thermal stress-driven slabbing of the crown of the drift. A UDEC equivalent Tptpmn rock mass will be developed and calibrated against large core compression testing results as discussed in Section 7.2.3.2 (see Section 2 for discussion of size effect on compressive strength in the Tptpmn). The UDEC model will be subjected to the measured temperatures and predictions made of the development of slabbing for the estimated in situ strength of the Tptpmn.

Thermal stress-induced degradation calculations will also be performed for the general Tptpmn case using the 3DEC and UDEC programs to examine the potential for both slabbing and block displacement during heating and cooling.

7.2.2.2 Modeling Approach for Time-Dependent Degradation

Time-Dependency of Fractures in Tptpmn
Fractures under constant shear and normal loads will develop stress concentrations in the asperities that comprise the joint roughness. It is conceivable that, over time, these asperities could undergo stress corrosion cracking, and shear, thereby reducing the roughness on the joint and its dilation. Therefore, in the worst case, the joint surfaces would be reduced to their condition of residual friction. A second mechanism may be shearing of solid rock bridges between non-persistent fracture branches, also due to a stress corrosion mechanism.

It is proposed that fracture degradation be addressed in the following ways:

- The potential for stress corrosion cracking and shearing of roughness and/or solid rock bridges from the joints will be examined through numerical analysis with the PFC

program. Static fatigue results from Tptpmn testing (see Section 6.2.4.3) will be used as a basis for a stress corrosion model.

- Worst case assumptions will be examined in the models–i.e., fractures will be assumed to be planar (no roughness) and will assume to completely cut the block in which they would normally terminate (i.e., no solid rock bridges).

- Comparison of the above two methods should give a picture of the conservatism inherent in worst case assumptions.

The data from static fatigue testing of the Tptpmn will be used as a basis for examination of time-dependency of roughness failure and its impact on the shear strength of discontinuities. To assess the likelihood of significant time-dependency of joint shear strength, the stress concentrations in roughness asperities, and its relation to their strength, needs to be examined for the major joint sets in the Tptpmn. Recall that there are four basic sets: two subvertical sets, the subhorizontal vapor phase partings, and the random set with intermediate dip. Of these sets, only the vapor phase partings are highly rough, with joint roughness coefficient values around 15 to 18. It is logical that only these joints would be particularly susceptible to strength degradation.

The PFC program will be used to conduct numerical shearing tests on simulated joints with roughness profiles derived from the Tptpmn mapping. Figure 37, Figure 38, and Figure 39 show a series of examples of simulated shearing tests on a rough joint using PFC, and the comparison of this model to the empirical joint shear behavior developed by Barton and Choubey (1977). Time-dependency in the PFC model can be examined using techniques similar to that discussed previously for modeling static fatigue in the Lac duBonnet granite, in which the particle bond strength is a function of the bond stress and time (as derived from calibration against lab static fatigue tests). The long-term shear and normal stress conditions existing on fractures will be estimated from the predictions of mining and thermally induced stresses.

The PFC modeling, including time dependence of the Tptpmn will be used to conduct a sensitivity study in which various levels of shear and normal stress are applied and held constant. The fracturing can assume both inherent roughness on the fracture surfaces as well as intact rock bridges between fracture segments. The potential for time-dependent damage will occur as a result of stress concentrations within the asperities along the fracture surface. The sensitivity study will identify what ratios of shear to normal stress will result in significant time-dependent damage. This will be used for comparison to the predicted stress conditions that have been calculated by regional thermomechanical modeling as discussed previously. If the models indicate a significant time dependence in the Tptpmn, then greater reliance will need to be placed on the base case of the seismic rockfall studies in which joints are assumed to be planar with no dilation on shearing. It is emphasized that the base case for rockfall simulations in the Tptpmn assumes planar joints with no short trace length roughness.

Time-Dependency in Lithophysal Rocks
The effect of time-dependent strength reduction in lithophysal rocks will be addressed through progressively detailed calculations as more data are obtained from laboratory testing.

Initial Bounding Analysis

Initial, worst-case analyses will examine the possible extent of caving and drip shield loading assuming the rock mass reaches its residual frictional strength. The most simplistic assumption, in the absence of any time-related strength degradation data are to assume that strength reduction can be related to a loss of cohesion of the material. The time-dependency aspects of this strength loss can eventually be related to static fatigue testing; however, it is initially instructive to simply determine how much strength loss is significant to rockfall. A parametric analysis can be conducted in which the cohesion is incrementally reduced while monitoring the resulting failure and rockfall. In this manner, it is possible to provide an initial bounding analysis that addresses the following points:

1. How much strength reduction (as a percentage of preexisting strength) is necessary for rockfall to occur – how does this relate to the results of laboratory static fatigue testing? How much time is expected for this process to occur?

2. What is the ultimate shape of the excavation when equilibrium is achieved? How is the bulking of the broken rock related to the shape of the blocks produced (i.e., the bulking factor), and the strength of the rock mass.

3. The static load on the drip shield or waste package, in absence of a drip shield.

Rigorous Approach

A second, and more rigorous approach to the problem was described previously in Section 6.2.4.3 in which a combination of laboratory static fatigue testing on Tptpmn and the PFC program to develop an understanding of static fatigue in lithophysal rocks. The strength time-dependency gained from this approach will be embedded within the PFC or other programs such as UDEC for parametric studies of the impact of static fatigue on tunnel failure mechanisms and the time for failure. It is envisaged that the impact of porosity on static fatigue will be used as the basis for the parametric studies. Predictions can be made as to the progression of damage and its impact on gravity-induced groundfall, with ultimate prediction of the equilibrium shape of the excavations and the static load distribution on the drip shields and waste packages.

Constant Horizontal   Velocity

PFC Model of
Rock and Joints

00266DC_044.ai
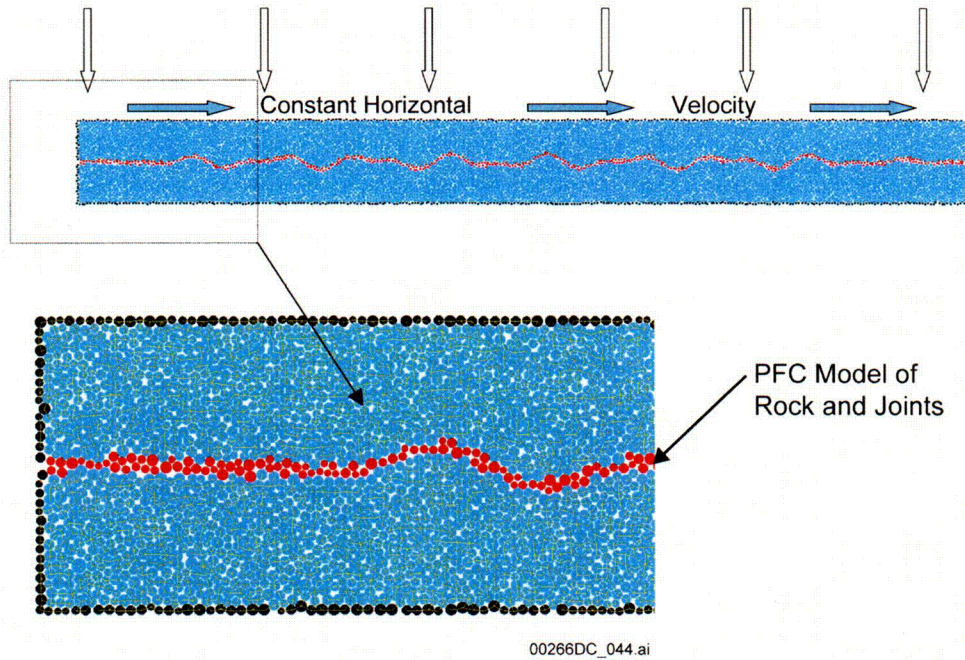
NOTE: Blue particles are given bonding properties that represent the solid Tptpmn; red particles
         represent the joint itself. Rock "sample" is subjected to normal stress and shear velocity to
         represent shear test.

Figure 37. PFC Model of a Rough Joint

Direction of Motion $\sigma_n = 0.65 \times UCS$ Microcracksfrom Shear Failure (Green)
                                                       and Tensile Failure (Red)

Rough Joint   Expanded View   Particle Contact Forces: Red = Tension
                                Black = Compression   Line Thickness is
                                Proportional to Force Magnitude
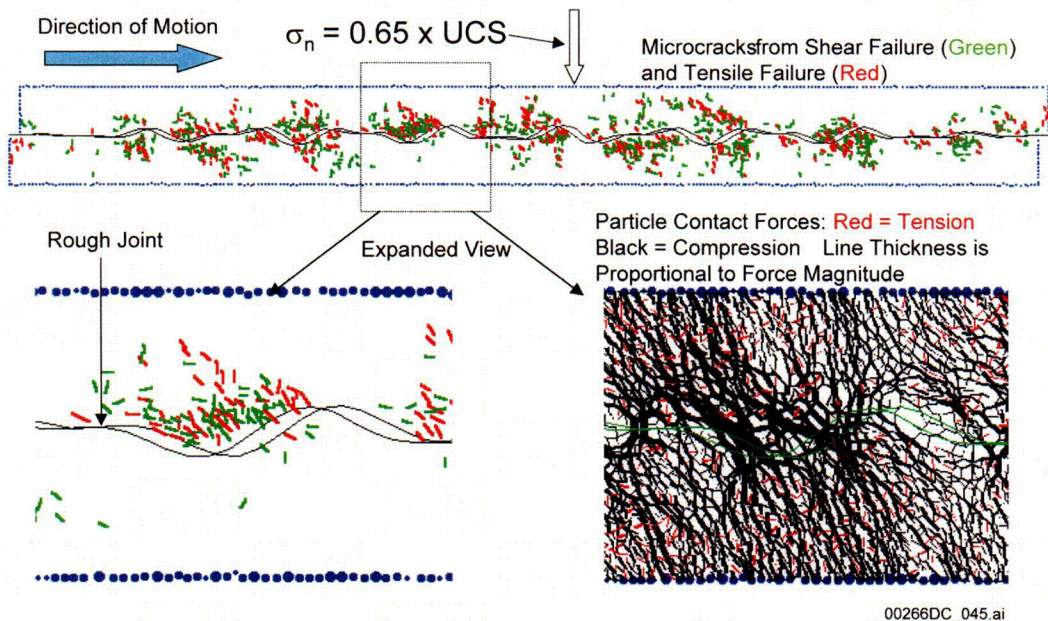
00266DC_045.ai

Figure 38.   Example of PFC Prediction of Damage Induced in Asperities for a Particular Case of Normal
              Stress as a Joint is Sheared

C05

Comparison to Barton-Bandis equations:

$$\tau = \sigma_n \tan\{JRC \log(JCS/\sigma_n)+\varnothing_r\}$$

$$d_n = JRC \log(JCS/\sigma_n)$$

Solid curves show values calculated by these equations for:

$$\varnothing_r = 24$$

$$JRC = 20$$

$$JCS = \sigma_c \text{ (UCS of solid)}$$

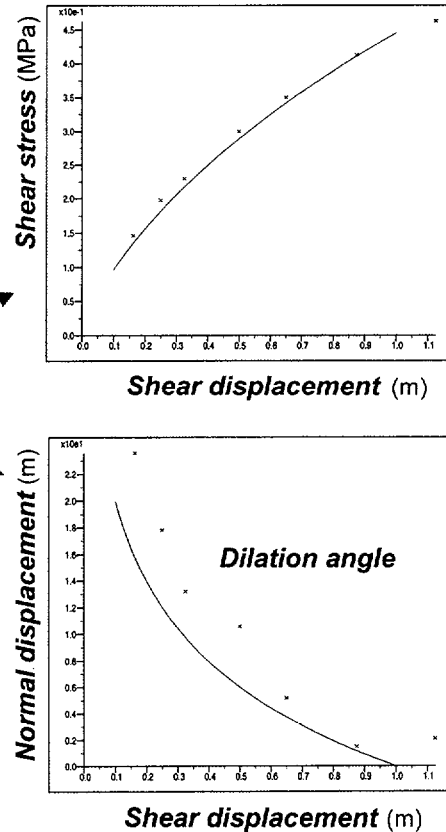Crosses show results from seven *PFC* simulations

Figure 39. Comparison of PFC Model Results to Barton-Bandis Empirical Joint Constitutive Model for Joint Shear and Normal Response

7.3 GROUND SUPPORT DESIGN AND EVALUATION

Ground support generally has one of three overall functions, depending on the type and quality of rock, and the stress conditions. First, it may be used to stabilize weak or overstressed ground and limit deformations to acceptable levels. Second, it may prevent gravitational loosening and fall of rock wedges in blocky, strong rock masses under low stress conditions. Finally, it can be used to maintain control of the rock surface in heavily fractured ground under low stress, by preventing unraveling or running. For repository emplacement drifts, ground support must:

- Ensure the stable conditions required for operational worker safety

- Limit the potential for rockfall[2] onto unprotected waste packages during the ventilated preclosure

- Allow for performance confirmation activities (which will include remote observation and possible testing functions), waste retrieval operations, and closure operations (which may include installation of permanent drip shields).

---

[2] Specifications for maximum size of rock particles contacting the waste package are not yet determined.

Furthermore, ground support needs to function throughout a repository preclosure period that could range from 50 to perhaps as high as 300 years. It is desired that the ground support require little of no maintenance due to the special requirements introduced by nuclear materials.

The following section describes the general methodology being developed for design of the ground support, and definition of support observation and maintenance over the retrieval period. This logic is currently under development and will be described in greater detail in a future Technical Data Report.

7.3.1 Current Drift Stability and Ground Support Function Under Gravitational Loading at Repository Depths–Predictions and Correspondence to Observations in the ESF and the ECRB Cross-Drift

7.3.1.1 Stress State

It is instructive to first examine the current stress conditions at the Yucca Mountain site, and their relation to the estimated rock mass strength and observations, particularly in the Tptpll within the ECRB, as a guide to ground support requirements.

The estimated stress conditions at the repository level are given in Table 4. The current repository design calls for emplacement drifts at a depth of approximately 300 m, oriented at N72°E. This orientation results in maximum and minimum stresses in the plane perpendicular to the axis of the drifts of about 7 MPa vertical and 3 MPa lateral. With these stress levels, the stress concentrations (assuming elastic behavior) at the springline will be approximately 18 MPa, and will be about 2 MPa at the crown (Figure 40). The stress levels at the floor will be the same.

7.3.1.2 Observations of Stability of the Tptpmn in the ESF and the ECRB

Due to the high uniaxial compressive strength of intact blocks of the Tptpmn, these stress concentrations will not result in any intact rock failure mechanisms. However, the fractured nature of the ground, and the presence of multiple joint sets, including a sub-horizontal set, results in the potential for gravity-induced wedge-type failures. In the ECRB Cross-Drift excavations, only a small number (less than 10) of wedge-type failures have occurred, with wedge sizes being roughly on the order of 1 ton or less. A larger number of loosened wedges (not fully documented) can be seen in the ESF, particularly in the area of the highly fractured zone. These wedges are formed by fracture sets 1 and 2 and the sub-horizontal vapor phase partings. These wedges were removed by the TBM during the excavation process, or by subsequent scaling operations; there are no known failures that have occurred at a later date. In the case of the Tptpmn, it appears reasonable that the primary function of the ground support is to prevent gravity fall of relatively small wedge sizes. Rockbolts of suitable length and spacing, supplemented by wire mesh perform well under these circumstances.

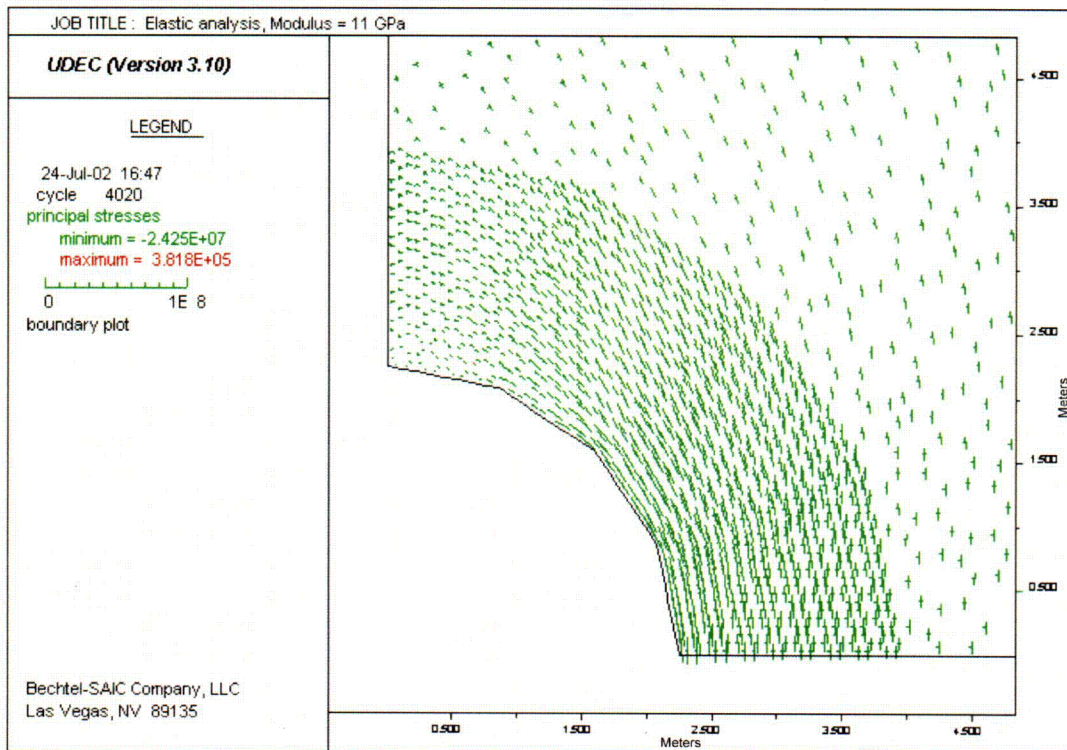Table 4. In Situ Stress Estimates at Yucca Mountain Site

Stress Component	Magnitude	Direction
σ_1	~0.023*depth (m)	Vertical
σ_2	$0.617^*\sigma_1$	N15°E
σ_3	$0.361^*\sigma_1$	N105°E

Source: WBS 1.2.3.2.7.3.4, WA-0065:QA:L

7.3.1.3 Observations of Stability in the Tptpll in the ECRB

Portions of both the ESF main tunnel and the ECRB are excavated in lithophysal rocks, and are generally quite stable using only rockbolts (Swellex™ and split sets) and wire mesh in the crown and walls as support. Observations in the Tptpll show obvious or intense small-scale fracture development at the tunnel springline, with the tunnel crown having less obvious fracture development. The origin of these fractures and the hackly appearance of the tunnel walls appears to be largely related to the action of the TBM cutters during the excavation process. However, observation of large (12 in. [30.5 cm]) diameter cores and the core hole walls drilled into the side walls of the tunnels indicate that there is a ubiquitous, natural fracture "fabric" within the Tptpll, with closely spaced (a few inches), irregular inter-lithophysal fractures of various orientations. These small-scale fractures often have vapor phase alteration on their surfaces, indicating their origin during the cooling process. A number of the large core holes drilled in the springline area show mining-induced, wall-parallel fractures that extend to a depth of about 12 to 18 in. (30.5 to 45.7 cm) from the tunnel wall. These fractures are not observed in similar holes in the Tptpul or Tptpmn.

The ground support function within this rock can be estimated from practical observation of the fracture density, as well as examination of the stress state in relation to the estimated rock mass strength. A simple parametric analysis of the yield zone around a tunnel in lithophysal rocks at 300 m depth can be conducted assuming the range of compressive strength data from the large core (10.5 in. [27 cm] diameter) Tptpul testing at Busted Butte. The relationship between uniaxial compressive strength and Young's modulus for this rock was shown in Figure 20.

JOB TITLE : Elastic analysis, Modulus = 11 GPa

UDEC (Version 3.10)

LEGEND

24-Jul-02 16:47
cycle   4020
principal stresses
    minimum = -2.425E+07
    maximum = 3.818E+05

0   1E 8
boundary plot

Bechtel-SAIC Company, LLC
Las Vegas, NV 89135

00266DC_051.ai

NOTE: Figure shows elastic rock at a depth of 300 m with vertical to horizontal stress ratio of 7 MPa to 3 MPa. Stress level is highest at the tunnel springline and lowest at the crown.
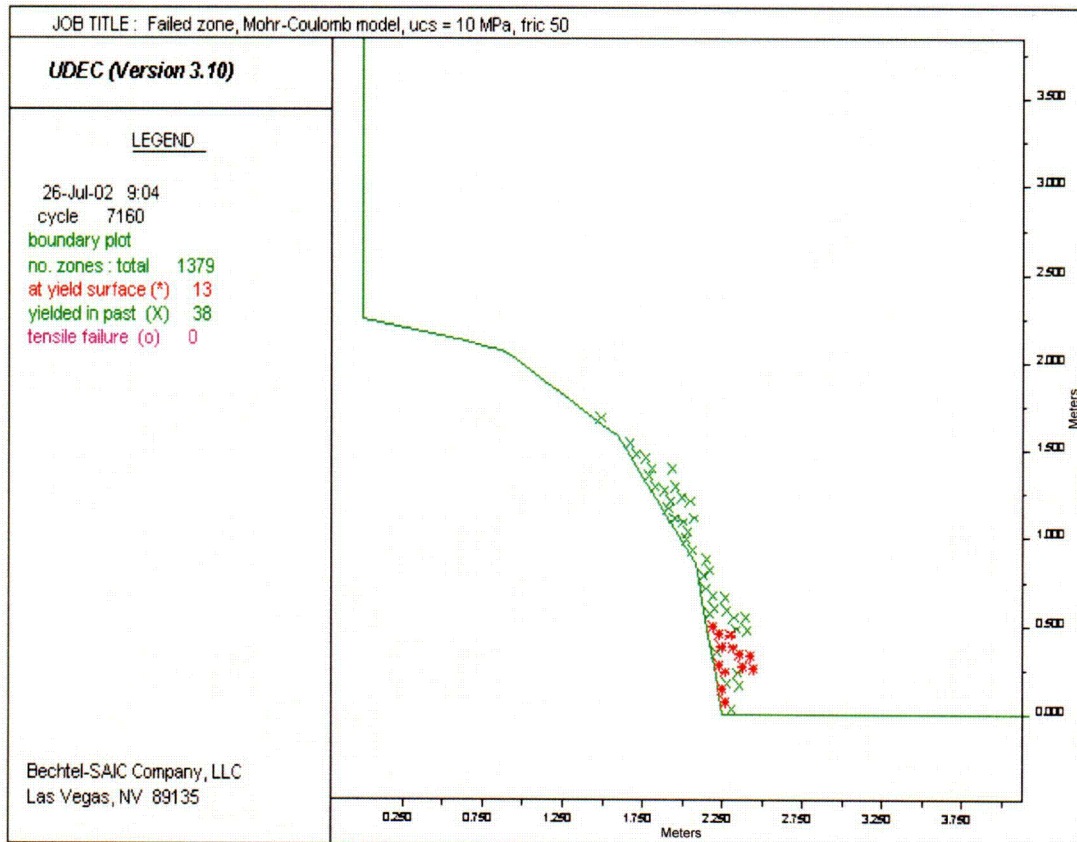
Figure 40. Mining-Induced Stress Around Quarter-Symmetry Tunnel

It is instructive to perform a simple modeling exercise in which the rock is assumed to behave as an elastic-plastic material with Mohr-Coulomb yield condition, and assuming the low end of the strength range presented in Figure 20 (uniaxial compressive strength of about 10 MPa, resulting in a cohesion of 1.28 MPa, assuming an angle of internal friction of 50°). For the stress state considered in Figure 40, an estimate of the extent of yield for an unsupported tunnel at repository depth can be made. Figure 41 shows the predicted stable tunnel with the extent of the failed zone for this case, which is about one-third to one-half of a meter at the tunnel springline (location of maximum stress difference), with no yield at the tunnel crown. This depth of failure is approximately the same as the depth of wall-parallel fracturing observed in the springline core holes as discussed above. The additional observation of a lack of mining-induced fracturing in the crown is also consistent with the calculations. Increasing the strength properties of the rock mass indicates that no yield is predicted when a uniaxial compressive strength of approximately 20 MPa (i.e., the maximum tangential stress at the springline) is reached. This observation shows that the general strength measurements determined thus far in the laboratory for lithophysal rocks is in reasonable agreement with observations in the ECRB – i.e., the level of yield predicted for the proposed rock strength is reasonable with respect to the observations of fracturing in the tunnel side walls.

Additionally, the tunnel is in equilibrium with only a few millimeters of total inward deformation, the maximum being at the roof centerline. These preliminary analyses point out

that the depth of yield under the current stress conditions is small, and overall equilibrium of the tunnel can be achieved without ground support. Therefore, under typical non-thermal or non-seismic loading conditions, the function of the ground support in the Tptpll is purely to retain small pieces of loosened or damaged material from gravity fall, and prevent any form of raveling response.
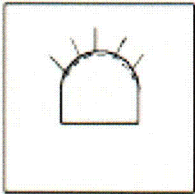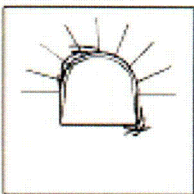

JOB TITLE : Failed zone, Mohr-Coulomb model, ucs = 10 MPa, fric 50

UDEC (Version 3.10)

LEGEND

26-Jul-02 9:04
cycle   7160
boundary plot
no. zones : total   1379
at yield surface (*)   13
yielded in past (X)   38
tensile failure (o)   0

Bechtel-SAIC Company, LLC
Las Vegas, NV 89135
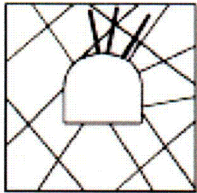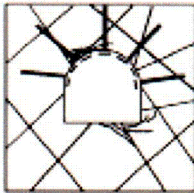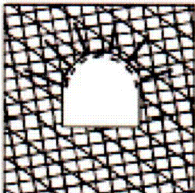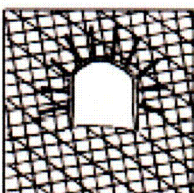
00266DC_034a.ai

NOTE: Under gravitational stress, the tunnel shows a small (approx. 0.5 m) yield zone in the side wall.

Figure 41. Yield Zone Around Tunnels in Tptpll

Figure 42 provides a check of the assumed ground support methods against typical industry-practice. This chart illustrates the role of ground support for the case of jointed rock (e.g., Tptpmn) and heavily fractured rock (e.g., Tptpll) under low stress conditions.

C07

	Low stress levels	High stress levels
Massive rock	Massive rock subjected to low in situ stress levels. No permanent support. Light support may be required for construction safety.	Massive rock subjected to high in situ stress levels. Pattern rockbolts or dowels with mesh or shotcrete to inhibit fracturing and to keep broken rock in place.
Jointed rock	Massive rock with relatively few discontinuities subjected to low in situ stress conditions. 'Spot' bolts located to prevent failure of individual blocks and wedges. Bolts must be tensioned. **Typical of Tptpmn**	Massive rock with relatively few discontinuities subjected to high in situ stress conditions. Heavy bolts or dowels, inclined to cross rock structure, with mesh or steel fibre reinforced shotcrete on roof and sidewalls.
Heavily jointed rock	Heavily jointed rock subjected to low in situ stress conditions. Light pattern bolts with mesh and/or shotcrete will control raveling of near surface rock pieces. **Typical of Tptpll**	Heavily jointed rock subjected to high in situ stress conditions. Heavy rockbolt or dowel pattern with steel fibre reinforced shotcrete. In extreme cases, steel sets with sliding joints may be required. Invert struts or concrete floor slabs may be required to control floor heave.

00266DC_035.ai

Source: Hoek 2000.

Figure 42. Typical Ground Support for Various Joint Densities and Stress Levels Showing Conditions Typical of the Tptpmn and Tptpll.

C08

7.3.2 Ground Support Design and Assessment Methodology

During the preclosure period, heat production from the emplaced waste packages will slowly raise the drift temperature and elevate the surrounding rock temperature, resulting in small stress changes around the excavations. The stress change will be dependent on a number of factors, including the initial waste canister heat output, the canister spacing, drift spacing, age of waste package, the amount of forced ventilation to be used, and the rock mass moduli. In any case, thermally induced stresses in the rock mass and ground support system are time-dependent. The *current* design basis for the preclosure ground support calls for a standard support of cement-grouted rockbolts and wire mesh with the potential for steel sets to be used where ground conditions dictate. It is recognized that:

- The current preclosure period of 50 to possibly as much as 300 years is a considerable length of time in terms of underground construction practice,

- Corrosion of the ground support will likely occur, and

- Depending on the length of the preclosure period, the type of ground support, and the degree of forced ventilation (to remove heat and moisture from the rock mass) the ground support may need to be maintained or supplemented at appropriate intervals.

The approach to preclosure ground support design and specification can be defined by the following methodology (Figure 43):

1. *Define the Support Operational Requirements* — Determine the requirements of the ground support during the preclosure period, including:

   a. Tunnel deformation limits (i.e., ensuring an operational envelope) for passage of vehicles and equipment, tilt limits for waste canisters and rails for remote retrieval, etc.

   b. Maximum rock particle size that can fall from in situ, thermal or seismically induced stresses and either strike the waste package and/or lie on rail or roadbed without compromising the ability to retrieve

   c. Support corrosion and degradation requirements,

   d. Impact of ground support on performance (i.e., the support may impact overall performance of the system). Preclosure use of ground support materials (cement and steel) depends on the postclosure effects of these materials on waste package corrosion and radionuclide transport. As currently planned, use of cementitious materials (e.g., concrete or shotcrete linings in emplacement drifts) will be minimized, use of exposed steel components (e.g., steel sets with steel lagging) will be also minimized, and loss of grout to fractures and lithophysae during rock bolt installation needs to be minimized.

2. *Define In Situ Conditions* — Includes rock mass in situ stresses, rock mass geotechnical characterization and properties. A detailed review of the rock mass characterization in the ESF and ECRB was given by Barton (2000).

3. *Initial Design of Suitable Ground Support Methods Under In Situ Conditions* — Use industry practice and empirical techniques (e.g., Barton 2000) to identify potentially suitable support methods.

4. *Detailed Mechanical and Environmental Examination of Support Suitability Under In Situ and Repository Loading Conditions* — Detailed design analysis of the deformation and possible failure extent and failure mode of the excavations considering range of input rock mass properties for the lithophysal and nonlithophysal rocks. Account for proper combinations of in situ, thermal, and seismic loads. Account for practical considerations in support design such as the fracture density and block sizes and the practicality of installation and servicing of the support methods. Consider environmental conditions including temperature, humidity and seepage. Consider the bounding scenarios and estimate the support loads and deformations and verify it fulfills operational requirements. Design calculations and considerations will be based on multiple approaches: computer modeling, empirical estimation, ESF and the ECRB experience, and drift scale testing and observation.

5. *Compare Proposed Support Methods to Repository Operational Requirements* — Identify possible support methods that fulfill the basic repository operational requirements. The operational requirements include definition of those structures, systems and components important to safety. Determine practicality of implementation of the support on a standard basis, including cost and maintainability. Estimate corrosion potential and life expectancy of support.

6. *Monitoring, Inspection and Maintenance Program* — Details of monitoring, inspection, and maintenance programs for the emplacement drifts will be developed as the program progresses from the conceptual design to the detailed design phase. DOE will specify structures, systems and components important to safety and natural and engineered barriers important to waste isolation. These structures, systems and components will be compatible with the risk-informed, performance-based approach embodied in 10 CFR Part 63. Parameters, measurements, and observations that are appropriate for inclusion in the performance confirmation program will be included in the detailed emplacement drift design based on their importance to repository performance and to addressing the detailed functional and quality level requirements of the ground support systems.

7.3.3 Methodology for Use of Numerical Models in Determining Ground Support Functions Under Repository Loading

A discussion is given below on possible ground support evaluation methods using numerical models. Why will numerical models be used for support evaluation? Normally, ground support is defined empirically. Rock mass classification schemes (e.g., the Q system) are used to define initial support methods and the tunnel construction management and engineer use observation, instrumentation, and practical judgment to adjust methods as necessary to fit actual conditions as

they unfold. Due to the obvious extenuating factors in the project (the thermal and seismic loading, the long time periods of support function, and the inability to easily observe and rehab the ground support) there is a greater reliance on detailed calculation and conservatism in the design. This implies the use of validated numerical modeling tools for examining rock mass yield and deformation, and the impact of rock mass variability on design requirements. As was shown in the overall resolution strategy diagram (Figure 22), the goal, prior to the ground support final specification, is to have a reasonable understanding of the in situ rock mass properties and their variability as input to numerical modeling. In this way, one can perform performance calculations that will predict rock mass response to the average and bounding rock quality conditions.
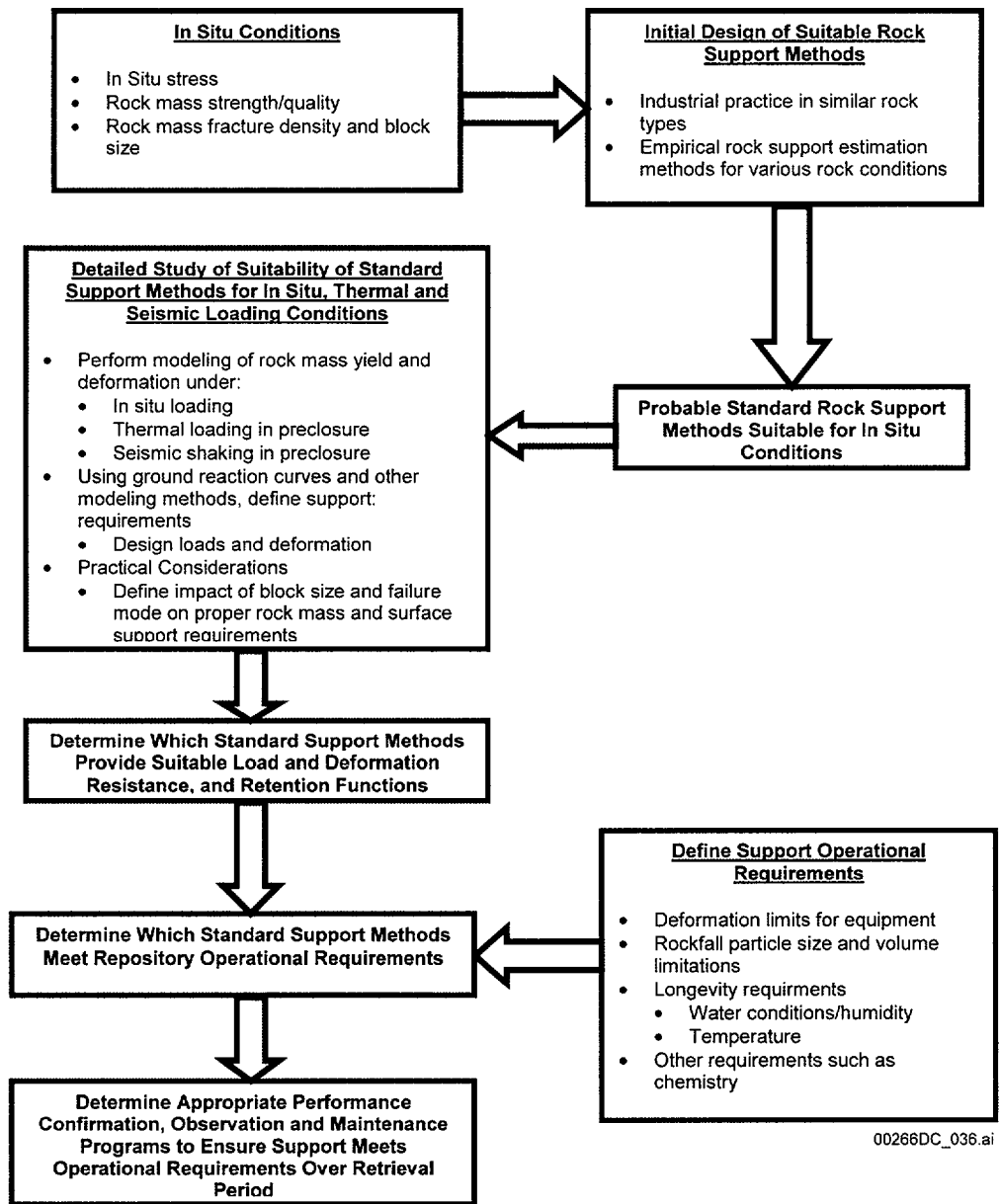

Figure 43. Ground Support Design and Assessment Methodology

7.3.3.1 Numerical Modeling of Rock Reinforcement

Numerical analyses of reinforced and unreinforced excavations will be performed for both the fracture-controlled Tptpmn as well as the lithophysal rocks.

Non-Lithophysal Rock
The design of rock support in the non-lithophysal rocks is based primarily on the geometric and surface properties of the fracturing. As discussed above, empirical methods (the Q system) will be used for the initial support specification in the Tptpmn. This support (which may consist of grouted or frictional bolts, wire mesh and perhaps fiber-reinforced shotcrete) will then be subjected to parametric numerical analysis using discontinuum numerical methods. Both the two-dimensional UDEC and three-dimensional 3DEC programs will be used for analysis of the support loads and rock mass yield and deformation when subjected to in situ, thermal and possible seismic loading over the preclosure period. The parametric analysis will include variation of fracture geometry and fracture properties, including cohesion, friction and dilation angles. It is convenient to utilize the three-dimensional synthetic fracture geometries (FracMAN) developed for the Tptpmn postclosure analysis as a basis for the ground support calculations. Here, a sensitivity study using various fracture realizations from this model can be used as input to the 3DEC program in the same way as discussed in Section 7.1. The models can be used to directly represent the ground support (Itasca 2002) and the application of transient loading from thermal and seismic sources. The rock mass temperature variation around the emplacement drifts with time during ventilated periods is obtained directly from the three-dimensional regional thermomechanical modeling. These temperatures will induce transient thermal stresses in the rock and expansion of support elements. The deformation of the rock and support loads can be determined directly from the model, and the factor of safety against failure for rock blocks determined in an automated fashion. It is possible that deterioration of the support elements due to corrosion can be included in the analyses through reduction of strength properties.

Lithophysal Rocks
As discussed previously, the lithophysal rocks are represented numerically using the UDEC program with mass properties calibrated to laboratory and in situ testing. The strength and stiffness properties of the rock mass are porosity dependent, resulting in a range of values that covers the range of in situ porosity variability. These properties provide the basic input data for thermomechanical sensitivity studies using the UDEC approach as described. As a secondary check on the analysis method, a more traditional continuum-based FLAC analysis assuming standard Mohr-Coulomb strength parameters will also be run.

A parametric analysis will be conducted in which various proposed rock support methods will be examined for the range of rock mass strength and stiffness properties. As with the 3DEC program, UDEC and FLAC allow various forms of rock support to be modeled directly within the analysis. The support load and deformation will be determined from the model as a function of time in the transient analyses. It is probable that both UDEC and FLAC approaches will be used here to define the general yield depth and deformation of the rock mass, and the expected overbreak or loosened zone and size of rock fragments that will need to be supported. This information will provide the performance requirements (load, deformability and block size to be supported) of the ground support.

The above calculations define the general operational conditions of the ground support based on the expected rock mass yield and deformation. This information is used as basic input to the final design of the ground support. The final design of the ground support is performed taking into account the results of these analyses and is combined with practical experience gained from working in the various rock units on site as well as similar conditions elsewhere. The experience to date has shown that excavations are quite stable with a minimum of ground support, as discussed previously. Experience has shown that in the nonlithophysal rocks (Tptpmn and Tptpln), the rock is moderately fractured but strong, with failure limited to the formation of an occasional small, removable wedge. Here, rockbolts are used to prevent loosening of wedges. In the Tptpul, the rock is weaker due to the uniformly distributed lithophysae, but only sparsely fractured, resulting in no observable yield and stable conditions under mining stress conditions. The Tptpll is heavily fractured with short length fractures between lithophysae, but with only widely spaced and relatively discontinuous fractures with lengths greater than a meter. The excavations are currently stable with support required only for retention of small pieces of loosened rock from the excavation periphery. In all of these rock types, the primary role of the support is a retention function under low stress conditions, and standard rockbolts and mesh prove successful. Ideal long-term support methods in ground such as the Tptpll would be those that provide a continuous lining and retention function such as fiber-reinforced shotcrete and bolts plated on the exterior surface. After selection of a number of alternative support methods, final selection will be based on the additional factors of the impact of support on postclosure performance and longevity of the support method.

7.3.3.2 Support Longevity and Other Items

An important aspect that will receive significant attention is the longevity of support elements. Currently, testing is underway to examine the general corrosion rates of steel support elements including rockbolts and steel sets subject to Yucca Mountain water chemistries. Additionally, grout-water interaction experiments relating to chemical effects on seepage water from rockbolt grouting are also underway. Additional aging studies on shotcrete including determination of carbonation rates may be conducted. This information will assist in understanding the longevity of ground support and its potential impacts on in-drift chemistry. Testing will also be performed on grout loss and rockbolt pull strength in lithophysal rocks.

Future examinations will include performance confirmation activities that will be conducted during construction of the repository. This will include geotechnical mapping and classification and determination of in situ property variability in the repository emplacement drifts. Testing of the mechanical properties of ground support and observation of performance during the preclosure period will be an integral part of performance confirmation.

INTENTIONALLY LEFT BLANK

8. SUMMARY

This document provides an approach to resolution of the geomechanically-related RDTME KTI agreements. The primary geomechanical issues are identified, and a program of geotechnical mapping and analysis, laboratory and in situ testing, in combination with numerical modeling are proposed for issue resolution.

Geomechanically-related KTI agreements (Appendix A) can be subdivided into five primary areas:

A. Rock mass properties and geotechnical characterization

1. Development of a basic understanding of how the structural characteristics of the repository host horizon impacts rock mass behavior and, consequently, the design and performance properties. This work can be used to establish a connection between geologic characteristics and their use in models and calculations.

2. Develop an understanding of the variability of geologic structure and, using the developments of the above item, identify how variability affects rock mass thermomechanical behavior.

3. Enhance the database of thermomechanical materials properties of repository rock units, including mechanical and thermal testing of lithophysal rocks, estimation of the mechanical properties of rock fractures, and determination of the time-dependent response of lithophysal rocks. Development or choice of proper constitutive models for the different distinct rock units is a portion of this effort.

B. Modeling

1. Determination or development of the proper type of modeling tools to use for sensitivity studies of excavation stability under gravitational, thermal and seismic shaking. Specific agreements cited in the KTI include:

a. Under what circumstances are continuum and discontinuum models appropriate?

b. Under what circumstances are two- and three-dimensional models appropriate?

c. Under what circumstances are assumptions of rock mass homogeneity or anisotropy appropriate?

2. Determination of the proper model boundary and initial conditions

a. Need to address the initial stress state for models and inclusion of thermally induced stress history from regional models applied to local scale models for problems such as rockfall

  b. Need to address special boundary conditions for dynamic analyses, including non-reflecting and free-field boundaries

  c. Need for development of preclosure and postclosure site-specific ground motion time histories

C. Seismic Stability

 1. Use of site-specific ground motions

 2. Use of appropriate dynamic models for estimation of rockfall induced by seismic shaking

 3. Methodology for inclusion of geologic structure and its variability into models for estimation of rockfall

D. Thermal and Long-term Degradation

 1. Need to examine potential for thermal-stress induced rockfall

 2. Need to examine impact of long-term static fatigue of the rock mass and its impact on drift degradation and rockfall

E. Ground Support and Drift Degradation

 1. Verification of the functional and operational requirements and specification of ground support during the preclosure period.

 2. Development of a plan for observation and maintenance of the ground support.

 3. Estimation of the effect of postclosure in situ, thermal and seismically induced stresses on the degradation and potential rockfall of the emplacement drifts. Included here is the potential effect of time-related static fatigue mechanisms in intact rock and joints.

9. REFERENCES

9.1 DOCUMENTS CITED

Albin, A.L.; Singleton, W.L.; Moyer, T.C.; Lee, A.C.; Lung, R.C.; Eatman, G.L.W.; and Barr, D.L. 1997. *Geology of the Main Drift - Station 28+00 to 55+00, Exploratory Studies Facility, Yucca Mountain Project, Yucca Mountain, Nevada.* Milestone SPG42AM3. Denver, Colorado: Bureau of Reclamation and U.S. Geological Survey. ACC: MOL.19970625.0096.

Barr, D.L, Moyer, T.C.; Singleton, W.L.; Albin, A.L.; Lung, R.C.; Lee, A.C.; Beason, S.C.; and Eatman, G.L.W. 1996. *Geology of the North Ramp — Stations 4+00 to 28+00, Exploratory Studies Facility, Yucca Mountain Project, Yucca Mountain, Nevada.* Denver, Colorado: U.S. Geological Survey. ACC: MOL.19970106.0496.

Barton, N. 2000. *A Review of the Site Characterization, and Suggestions for a Site Specific Method of Design for Long Term Ground Control at the Yucca Mountain Project.* 20001174. Oslo, Norway: Norwegian Geotechnical Institute. TIC: 248878.

Barton, N. and Choubey, V. 1977. "*The Shear Strength of Rock Joints in Theory and Practice.*" *Rock Mechanics, 10,* (1-2), 1-54. New York, New York: Springer-Verlag. TIC: 218374.

Barton, N.; Lien, R.; and Lunde, J. 1974. "*Engineering Classification of Rock Masses for the Design of Tunnel Support.*" *Rock Mechanics, 6,* (4), 189-236. New York, New York: Springer-Verlag. TIC: 219995.

Beason, S.C.; Turlington, G.A.; Lung, R.C.; Eatman, G.L.W.; Ryter, D.; and Barr, D.L. 1996. *Geology of the North Ramp - Station 0+60 to 4+00, Exploratory Studies Facility, Yucca Mountain Project, Yucca Mountain, Nevada.* Denver, Colorado: U.S. Geological Survey. ACC: MOL.19970106.0449.

Bieniawski, Z.T. 1989. *Engineering Rock Mass Classifications.* New York, New York: John Wiley & Sons. TIC: 226350.

Board, M. Linden, A.; and Zhu, M. 2002. *Design Evolution Study—Underground Layout.* TDR-MGR-MG-000003 REV 00. Las Vegas, Nevada: Bechtel SAIC Company. ACC: MOL.20020429.0023.

Brechtel, C.E.; Lin, M.; Martin, E.; and Kessel, D.S. 1995. *Geotechnical Characterization of the North Ramp of the Exploratory Studies Facility.* SAND95-0488/1 and 2. Two volumes. Albuquerque, New Mexico: Sandia National Laboratories. ACC: MOL.19950502.0004; MOL.19950502.0005.

Broxton, D.E.; Chipera, S.J.; Byers, F.M., Jr.; and Rautman, C.A. 1993. *Geologic Evaluation of Six Nonwelded Tuff Sites in the Vicinity of Yucca Mountain, Nevada for a Surface-Based Test Facility for the Yucca Mountain Project.* LA-12542-MS. Los Alamos, New Mexico: Los Alamos National Laboratory. ACC: NNA.19940224.0128.

BSC 2001. *Drift Degradation Analysis*. ANL-EBS-MD-000027 REV 01 ICN 01. Las Vegas, Nevada: Bechtel SAIC Company. ACC: MOL.20011029.0311.

BSC 2002. *Thermal Conductivity of the Potential Repository Horizon Model Report*. MDL-NBS-GS-000005 REV 00. Las Vegas, Nevada: Bechtel SAIC Company. ACC: MOL.20020923.0167.

Buesch, D.C.; Spengler, R.W.; Moyer, T.C.; and Geslin, J.K. 1996. *Proposed Stratigraphic Nomenclature and Macroscopic Identification of Lithostratigraphic Units of the Paintbrush Group Exposed at Yucca Mountain, Nevada*. Open-File Report 94-469. Denver, Colorado: U.S. Geological Survey. ACC: MOL.19970205.0061.

Byers, F.M., Jr.; Carr, W.J.; Orkild, P.P.; Quinlivan, W.D.; and Sargent, K.A. 1976. *Volcanic Suites and Related Cauldrons of Timber Mountain-Oasis Valley Caldera Complex, Southern Nevada*. Professional Paper 919. Washington, D.C.: U.S. Geological Survey. TIC: 201146.

Christiansen, R.L.; Lipman, P.W.; Carr, W.J.; Byers, F.M., Jr.; Orkild, P.P.; and Sargent, K.A. 1977. "The Timber Mountain-Oasis Valley Caldera Complex of Southern Nevada." *Geological Society of America Bulletin, 88,* (7), 943-959. [Boulder, Colorado]: Geological Society of America. TIC: 201802.

CRWMS M&O 1997. *Confirmation of Empirical Design Methodologies*. BABEE0000-01717-5705-00002 REV 00. Las Vegas, Nevada: CRWMS M&O. ACC: MOL.19980219.0104.

CRWMS M&O 1998a. *Probabilistic Seismic Hazard Analyses for Fault Displacement and Vibratory Ground Motion at Yucca Mountain, Nevada*. Milestone SP32IM3, September 23, 1998. Three volumes. Las Vegas, Nevada: CRWMS M&O. ACC: MOL.19981207.0393.

CRWMS M&O 1998b. *Geology of the Exploratory Studies Facility Topopah Spring Loop*. BAB000000-01717-0200-00002 REV 01. Las Vegas, Nevada: CRWMS M&O. ACC: MOL.19980415.0283.

CRWMS M&O 1999. *TBV-361 Resolution Analysis: Emplacement Drift Orientation*. B00000000-01717-5705-00136 REV 00. Las Vegas, Nevada: CRWMS M&O. ACC: MOL.19990802.0316.

Day, W.C.; Dickerson, R.P.; Potter, C.J.; Sweetkind, D.S.; San Juan, C.A.; Drake, R.M., II; and Fridrich, C.J. 1998. *Bedrock Geologic Map of the Yucca Mountain Area, Nye County, Nevada*. Geologic Investigations Series I-2627. Denver, Colorado: U.S. Geological Survey. ACC: MOL.19981014.0301.

DOE (U.S. Department of Energy) 2002. *Yucca Mountain Science and Engineering Report*. DOE/RW-0539, Rev. 1. Washington, D.C.: U.S. Department of Energy, Office of Civilian Radioactive Waste Management. ACC: MOL.20020404.0042.

Eatman, G.L.W.; Singleton, W.L.; Moyer, T.C.; Barr, D.L.; Albin, A.L.; Lung, R.C.; and Beason, S.C. 1997. *Geology of the South Ramp - Station 55+00 to 78+77, Exploratory Studies Facility, Yucca Mountain Project, Yucca Mountain, Nevada.* Denver, Colorado: U.S. Department of Energy. ACC: MOL.19980127.0396.

Gibson, J.D.; Shephard, L.E.; Swan, F.H.; Wesling, J.R.; and Kerl, F.A. 1990. "Synthesis of Studies for the Potential of Fault Rupture at the Proposed Surface Facilities, Yucca Mountain, Nevada." *High Level Radioactive Waste Management, Proceedings of the International Topical Meeting, Las Vegas, Nevada April 8-12, 1990.* 1, 109-116. La Grange Park, Illinois: American Nuclear Society. TIC: 202058.

Hoek, E. 2000. "Rock Engineering: Course Notes." Practical Rock Engineering. Toronto, Ontario: Rocscience Inc. Accessed Wednesday, November 13, 2002. TIC: 253544. http://www.rockscience.com/roc/Hoek/Hoeknotes2000.htm.

Itasca Consulting Group. 2002. *Itasca Software–Cutting Edge Tools for Computational Mechanics.* Minneapolis, Minnesota: Itasca Consulting Group. TIC: 252592.

Kicker, D.C.; Martin, E.R.; Brechtel, C.E.; Stone, C.A.; and Kessel, D.S. 1997. *Geotechnical Characterization for the Main Drift of the Exploratory Studies Facility.* SAND95-2183. Albuquerque, New Mexico: Sandia National Laboratories. TIC: 227586.

Kirsten, H.A.D. 1988. "Discussion on Q-System." *Rock Classification Systems for Engineering Purposes, Symposium held in Cincinnati, Ohio, June 25, 1987.* Kirkaldie, L., ed. Pages 85-88. Philadelphia, Pennsylvania: American Society for Testing and Materials. TIC: 221986.

Lajtai, E.Z., Schmidtke, R.H., and Bielus, L.P. *The Effect of Water on the Time-dependent Deformation and Fracture of a Granite.* Int. J. Rock Mech. Min. Sci.. Vol. 24, No. 4, pp. 247 to 255, 1987. TIC: 236692.

Lipman, P.W.; Christiansen, R.L.; and O'Connor, J.T. 1966. *A Compositionally Zoned Ash-Flow Sheet in Southern Nevada.* Professional Paper 524-F. Washington, D.C.: U.S. Geological Survey. TIC: 219972.

Mongano, G.S.; Singleton, W.L.; Moyer, T.C.; Beason, S.C.; Eatman, G.L.W.; Albin, A.L.; and Lung, R.C. 1999. *Geology of the ECRB Cross Drift - Exploratory Studies Facility, Yucca Mountain Project, Yucca Mountain, Nevada.* [Deliverable SPG42GM3]. Denver, Colorado: U.S. Geological Survey. ACC: MOL.20000324.0614.

NRC (U.S. Nuclear Regulatory Commission) 2000. *Issue Resolution Status Report Key Technical Issue: Repository Design and Thermal-Mechanical Effects.* Rev. 3. Washington, D.C.: U.S. Nuclear Regulatory Commission. ACC: MOL.20010201.0256.

Ortiz, T.S.; Williams, R.L.; Nimick, F.B.; Whittet, B.C.; and South, D.L. 1985. *A Three-Dimensional Model of Reference Thermal/Mechanical and Hydrological Stratigraphy at Yucca Mountain, Southern Nevada.* SAND84-1076. Albuquerque, New Mexico: Sandia National Laboratories. ACC: MOL.19980602.0331.

Potyondy, D. and Cundall, P. 2001. *The PFC Model for Rock: Predicting Rock-Mass Damage at the Underground Research Laboratory.* Itasca Consulting Group, Inc., Report To Atomic Energy of Canada Limited (AECL), March. Issued as Ontario Power Generation. Nuclear Waste Management Division Report No. 06819-REP-01200-10061-R00. Minneapolis, Minnesota: Itasca Consulting Group.

Price, R.H. 1986. *Effects of Sample Size on the Mechanical Behavior of Topopah Spring Tuff.* SAND85-0709. Albuquerque, New Mexico: Sandia National Laboratories. ACC: NNA.19891106.0125.

Price, R.H.; Nimick, F.B.; Connolly, J.R.; Keil, K.; Schwartz, B.M.; and Spence, S.J. 1985. *Preliminary Characterization of the Petrologic, Bulk, and Mechanical Properties of a Lithophysal Zone Within the Topopah Spring Member of the Paintbrush Tuff.* SAND84-0860. Albuquerque, New Mexico: Sandia National Laboratories. ACC: NNA.19870406.0156.

Sawyer, D.A.; Fleck, R.J.; Lanphere, M.A.; Warren, R.G.; Broxton, D.E.; and Hudson, M.R. 1994. *"Episodic Caldera Volcanism in the Miocene Southwestern Nevada Volcanic Field: Revised Stratigraphic Framework, 40Ar/39Ar Geochronology, and Implications for Magmatism and Extension."* Geological Society of America Bulletin, 106, (10), 1304-1318. Boulder, Colorado: Geological Society of America. TIC: 222523.

Schuraytz, B.C.; Vogel, T.A.; and Younker, L.W. 1989. "Evidence for Dynamic Withdrawal from a Layered Magma Body: The Topopah Spring Tuff, Southwestern Nevada." *Journal of Geophysical Research, 94,* (B5), 5925-5942. Washington, D.C.: American Geophysical Union. TIC: 225936.

Scott, R.B. 1990. "Tectonic Setting of Yucca Mountain, Southwest Nevada." Chapter 12 of *Basin and Range Extensional Tectonics Near the Latitude of Las Vegas Nevada.* Wernicke, B.P., ed. Memoir 176. Boulder, Colorado: Geological Society of America. TIC: 222540.

Scott, R.B. and Bonk, J. 1984. *Preliminary Geologic Map of Yucca Mountain, Nye County, Nevada, with Geologic Sections.* Open-File Report 84-494. Denver, Colorado: U.S. Geological Survey. ACC: HQS.19880517.1443.

Young, R.P. and Collins, D.S. 1997. *Acoustic Emission/Microseismicity Research at the Underground Research Laboratory,* Canada. AECL Report Series, 00670367. Ontario, Canada: Atomic Energy of Canada, Ltd. TIC: 253464.

9.2   CODES, STANDARDS, REGULATIONS, AND PROCEDURES

10 CFR 63. Energy: Disposal of High-Level Radioactive Wastes in a Geologic Repository at Yucca Mountain, Nevada. Readily available.

9.3   SOURCE DATA, LISTED BY DATA TRACKING NUMBER

GS990408314224.004. Full-Periphery Geologic Maps for Station 10+00 to 15+00, ECRB Cross Drift. Submittal date: 09/09/1999.

9.4   SOFTWARE CODES

Software code: 3DEC. V2.0. 10025-2.0-00.

Software Code: FLAC V3.5. V 3.5. PC. 10167-3.5-00.

Software code: FracMAN. V.2.511. PC Windows NT. 10114-2.511-00.

Software Code: PFC 2D. V.2.0. PC. 10828-2.0-00.

Software Code: PFC 3D. V.2.0. PC. 10830-2.0-00.

Software code: UDEC V3.0. V 3.0. PC. 10173-3.0-00.

INTENTIONALLY LEFT BLANK

OVERVIEW OF THE RESOLUTION STRATEGY FOR
EACH GEOMECHANICALLY-RELATED KTI AGREEMENT

INTENTIONALLY LEFT BLANK

APPENDIX A: OVERVIEW OF THE RESOLUTION STRATEGY FOR EACH GEOMECHANICALLY-RELATED KTI AGREEMENT

The relevant geomechanically-related KTI agreements and an overview of the resolution strategy for each of the agreements covered by this document are listed below. Details of the overall resolution strategy are given in Sections 5 and 6 of this report.

RDTME 3.02

Provide the critical combinations of in-situ, thermal, and seismic stresses, together with their technical bases, and their impacts on ground support performance. The DOE will examine the critical combinations of in-situ, thermal, and seismic stresses, together with their technical bases and their impacts on preclosure ground support performance. These results will be documented in a revision to Ground Control for Emplacement Drifts for SR, ANL-EBS-GE-000002 (or other document) supporting any potential license application. This is expected to be available to NRC in FY 2003.

General Approach:

Numerical sensitivity studies will be conducted using continuum and discontinuum methods that examine the combined effect of preclosure stress conditions. The following work will be used to address this issue.

- Laboratory and in situ testing will be used to define strength and deformability property ranges for lithophysal rocks. Lithophysal mapping and numerical extrapolation will be used to define impact of lithophysal variability on rock mass properties.

- Field mapping of joint geometry and roughness characteristics will be used to define rock block geometries. Laboratory testing will be conducted to determine joint surface characteristics using direct shear testing. Fracture geometries will be developed using FracMAN fracture modeling program.

- Numerical modeling sensitivity studies will be performed using 3DEC, UDEC, and FLAC programs to examine yield and deformation in lithophysal and non-lithophysal tunnels. Models will use thermal, in situ, and seismic stresses in preclosure to examine effectiveness of ground support in preventing rockfall. Models will account for range of estimated properties of rock mass and fractures, as well as variability in joint geometries.

RDTME 3.04

Provide in the Design Parameter Analysis Report (or some other document) site-specific properties of the host rock, as a minimum those included in the NRC handout, together with the spatial and temporal variations and uncertainties in such properties, as an update to the information contained in the March 1997 Yucca Mountain Site Geotechnical Report. The DOE will: (1) evaluate the adequacy of the currently available measured and derived data to support the potential repository licensing case and identify areas where available data may

warrant additional field measurements or testing to reduce uncertainty. DOE will provide a design parameters analysis report (or other document) that will include the results of these evaluations, expected to be available to the NRC in FY 2002; and (2) acquire data and/or perform additional analyses as necessary to respond to the needs identified in 1 above. The DOE will provide these results prior to any potential license application.

General Approach:

- The current rock properties data base is reviewed in Appendix B, and an assessment of thermomechanical data needs made.

- Areas identified that require additional data include:

  - Thermomechanical properties of the lithophysal rocks, including strength, deformability and thermal properties

  - Static fatigue properties of lithophysal and non-lithophysal rocks

  - Shear stress-displacement behavior of joints in the non-lithophysal units

  - Description of large-scale roughness in joints in the non-lithophysal units and variation of lithophysae shape, size and porosity in the lithophysal rocks.

- A laboratory and field testing program and an additional geological characterization program have been developed to gather these data. Underground and surface mapping will be combined with borehole logging to define the variability of geologic structure within the repository block. A laboratory and field testing program for lithophysal rocks is underway at Sandia National Laboratories. Tests include large (12-in. [30.5-cm]) diameter core and in situ slot compression testing to obtain compressive strength and deformability. Direct shear testing on 12-in. (30.5-cm) core fractures is underway at the United States Bureau of Reclamation (USBR) laboratories in Denver to obtain shear constitutive behavior. Static fatigue testing of a small number of lithophysal and non-lithophysal samples is also planned at the USBR laboratories. Calibration of the PFC model is planned to allow exploration of impact of lithophysae variability on properties.

- Design parameters sensitivity analyses will be used to examine effects of property variations on ground support and drift degradation. A revision of *Drift Degradation Analyses* (BSC 2001) will be completed in FY 2003, and *Ground Control Analysis for Emplacement Drifts* will be completed in the first quarter of FY 2004.

RDTME 3.05

Provide the Rock Mass Classification Analysis (or some other document) including the technical basis for accounting for the effects of lithophysae. The DOE will provide a rock mass classification analysis (or other document),

including the technical basis for accounting for the effects of lithophysae, expected to be available to NRC in FY 2002.

General Approach:

The effect of lithophysae on rock mass properties will be determined directly via:

- Testing of large cores in the laboratory

- In situ compression testing in Tptpul and Tptpll

- Validation of the PFC numerical model against these data to provide a predictive tool capable of modeling the stress-strain response of lithophysal rock. Geologic mapping and geometric description of the lithophysae as a function of depth in the ECRB will provide direct descriptions of lithophysal porosity, shape and size variability. This mapping will provide basis of extrapolation of lithophysal variability impacts on rock properties via PFC.

- Testing, supplemented by model extrapolations will be used to define the variability of properties of the lithophysal rocks.

- This analysis will be included in two documents: a revision of *Drift Degradation Analyses* (BSC 2001) in FY 2003, and *Fracture and Lithophysae Characteristics of the Repository Host Horizon* in the first quarter of FY 2004.

RDTME 3.06

Provide the design sensitivity and uncertainty analyses of the rock support system. The DOE will prepare a scoping analysis to determine the significance of the input parameters for review by NRC staff by August 2002. Once an agreed set of significant parameters has been determined by the DOE and NRC staff, the DOE will prepare an analysis of the sensitivity and uncertainty of the preclosure rock support system to design parameters in a revision to Ground Control for Emplacement Drifts for SR, ANL-EBS-GE-000002 (or other document) supporting any potential license application. This is expected to be available to NRC in FY 2003.

General Approach:

Sensitivity studies of ground support will be conducted for non-lithophysal and lithophysal rocks using continuum and discontinuum numerical methods.

- Ground support requirements (maximum rockfall size, environmental conditions, longevity, etc.) developed as part of project System Design Description.

- Initial ground support methods will be defined empirically. Value Engineering studies will be used to determine candidate support methods for further analysis.

- Input rock mass, fracture and support data parameters are derived from lab and in situ testing and numerical extrapolation, geologic mapping, in situ support testing, and literature – see discussion for RDTME 3.04 for a discussion of rock properties.

- Modeling sensitivity studies will be primarily discontinuum modeling using range of input properties and stress conditions in preclosure. Several methods will be used to examine support design, including direct modeling of the ground support, and use of the ground reaction curve method.

- Loading conditions in preclosure will include in situ, thermal and seismic stresses.

- Scoping analyses will be presented in *Ground Control Analysis for Emplacement Drifts* in the first quarter of FY 2004.

RDTME 3.07

The DOE should account for the effect of sustained loading on intact rock strength or provide justification for not accounting for it. The DOE will assess the effects of sustained loading on intact rock strength. The DOE will provide the results of this assessment in a design parameters analysis report (or other document), expected to be available to NRC in FY 2002.

General Approach:

The effect of sustained loading will be addressed through a combination of rock mechanics testing and numerical modeling. The following work is planned:

- Estimates of static fatigue strength of non-lithophysal and lithophysal rock samples will be determined from laboratory and limited time-scale in situ tests. Lab tests on 6 to 12 in. (15.2 to 30.5 cm) diameter cores tested at about 90°C. Load developed in steps from approx. 50 percent peak strength to 90 percent.

- Estimated time-to-failure will be determined as a function of percent of the uniaxial compression strength and will be used with modeled stresses to determine estimated time to failure for rock mass. Estimated time-to-failure can be incorporated into simple constitutive model to allow time-related degradation to occur.

- Joint shear strength degradation will be developed using static fatigue testing of non-lithophysal cores. The PFC model will be used to conduct numerical shear loading in which time-to-failure as a function of stress is accounted for in strength logic in model. Will estimate whether this mode of failure could have impact on long-term degradation in non-lithophysal materials.

- Will be addressed in the revision of *Drift Degradation Analyses* (BSC 2001) as long-term fatigue data becomes available.

RDTME 3.08

Provide the design sensitivity and uncertainty analyses of the fracture pattern (with respect to Subissue 3, Component 1). The DOE will provide sensitivity and uncertainty analysis of fracture patterns (based on observed orientation, spacing, trace length, etc) on the preclosure ground control system design in a revision to Ground Control for Emplacement Drifts for SR, ANL-EBS-GE-000002 (or other document) supporting any potential license application. This is expected to be available to NRC in FY 2003.

General Approach:

A detailed analysis of the fracture patterns in the non-lithophysal and lithophysal rocks will be performed. Work effort will include:

- Data base will include existing ECRB and ESF detailed line surveys and full periphery mapping. These data include 1 m or longer trace lengths.

- Fracture geometry will be analyzed by using the FracMAN program to develop structural input to rockfall analysis and by creating a 100-m cube representative fractured rock mass. Tunnel centroids within representative volume will be determined randomly.

- Back-checking output from FracMAN against actual detailed line survey statistics. Creating full periphery trace maps from FracMAN to check against actual maps for practical geologic check.

- Fracture geometries will be input to 3DEC discontinuum modeling package that defines block geometries from non-persistent fracture systems. 3DEC will be used to determine rock mass stability. Many runs with various fracture geometries will be conducted to determine sensitivity of preclosure response to fracture patterns.

- This work will be documented in two places: the revision of *Drift Degradation Analyses* (BSC 2001) in FY 2003, and *Fracture and Lithophysae Characteristics of the Repository Host Horizon* in the first quarter of FY 2004.

RDTME 3.09

Provide appropriate analysis that shows rock movements in the invert are either controlled or otherwise remain within the range acceptable to provide for retrieval and other necessary operations within the deposal drifts. DOE will provide appropriate analysis that shows rock movements in the floor of the emplacement drift are within the range acceptable for preclosure operations. The analysis results will be provided in a revision to Ground Control for Emplacement Drifts for SR, ANL-EBS-GE-000002 (or other document) supporting any potential license application. This is expected to be available to NRC in FY 2003.

General Approach:

- Numerical modeling of excavation stability under in situ, thermal and seismic loading will examine deformation of the tunnel.

- An output of these studies will be drift periphery deformations, which will be examined with reference to opening performance specifications for emplacement operations and retrieval.

- Work will be documented in *Ground Control Analysis for Emplacement Drifts* in the first quarter of FY 2004.

RDTME 3.10

Provide technical basis for the assessment that two-dimensional modeling of emplacement drifts is considered to be adequate, considering the fact that neither the in-situ stress field nor the principle fracture orientation are parallel or perpendicular to emplacement drift orientation. The DOE will provide the technical bases for the modeling methods used in ground control analysis in a revision to Ground Control for Emplacement Drifts for SR, ANL-EBS-GE-000002 (or other document) supporting any potential license application. This is expected to be available to NRC in FY 2003.

General Approach:

- This assessment will be provided as part of the revision of *Drift Degradation Analyses* (BSC 2001) in FY 2003.

- Three-dimensional modeling will be used for rockfall and ground support studies in the non-lithophysal rocks as the mechanical response is expected to be fracture controlled, and thus three-dimensional and anisotropic.

- It will be justified that the lithophysal rock is effectively isotropic and homogenous due to the roughly uniform distribution of lithophysae within the unit. This results in ability to use two-dimensional models in this case.

RDTME 3.11

Provide continuum and discontinuum analyses of ground support system performance that take into account long-term degradation of rock mass and joint strength properties. The DOE will justify the preclosure ground support system design (including the effects of long-term degradation or rock mass and joint strength properties) in a revision to Ground Control for Emplacement Drifts for SR, ANL-EBS-GE-000002 (or other document) supporting any potential license application. This is expected to be available to NRC in FY 2003.

General Approach:

- Both two-dimensional and three-dimensional discontinuum and continuum models will be used for rockfall and long-term strength degradation studies. It is questionable if the preclosure period (50 to perhaps as much as 300 years) is considered "long-term" in terms of strength degradation.

- See RDTME 3.07 above for description of strength degradation measurement strategy.

- The 3DEC, UDEC and PFC discontinuum programs and FLAC continuum programs will be used for thermomechanical calculations. Estimates of static fatigue effects on joint and rock mass strength will be accounted for in constitutive models for joints and the rock mass. It is assumed that ground support systems have preclosure functionality, and therefore long-term degradation does not necessarily impact ground support unless static fatigue testing indicates exceptionally short times to failure.

- Work will be documented in *Ground Control Analysis for Emplacement Drifts* in the first quarter of FY 2004.

RDTME 3.12

Provide dynamic analyses (discontinuum approach) of ground support system performance using site-specific ground motion history as input. The DOE will provide appropriate analyses to include dynamic analyses (discontinuum approach) of preclosure ground support systems, using site-specific ground motion time histories as input, in a revision to Ground Control for Emplacement Drifts for SR, ANL-EBS-GE-000002 (or other document) supporting any potential license application. This is expected to be available to NRC in FY 2003.

General Approach

- Approach to dynamic analysis of rockfall documented in the RDTME KTI Agreement Resolution Document.

- Both two-dimensional (UDEC, discontinuum, lithophysal) and three-dimensional (3DEC, discontinuum for non-lithophysal) dynamic analysis methods will be used for preclosure and postclosure rockfall analyses.

- Site-specific ground motions developed from *Probabilistic Seismic Hazard Analyses for Fault Displacement and Vibratory Ground Motion at Yucca Mountain, Nevada* (CRWMS M&O 1998). The Appendix 7 meeting with NRC in August of 2002 described ground motion development methodology.

- Dynamic analyses will be completed for preclosure and postclosure time histories. Rockfall documented in terms of rock particle size distribution, velocity and impact location.

- The results will be documented in the revision of *Drift Degradation Analyses* (BSC 2001) in FY 2003 and in *Ground Control Analysis for Emplacement Drifts* in the first quarter of FY 2004.

RDTME 3.13

Provide technical justification for boundary conditions used for continuum and discontinuum modeling used for underground facility design. The DOE will provide the technical justification for boundary conditions used in modeling for preclosure ground control analyses, in a revision to Ground Control for Emplacement Drifts for SR, ANL-EBS-GE-000002 (or other document) supporting any potential license application. This is expected to be available to NRC in FY 2003.

General Approach:

- *Ground Control Analysis for Emplacement Drifts* and the revision of *Drift Degradation Analyses* (BSC 2001) will have justification for boundary and initial conditions used in all modeling.

- Dynamic analyses will use site-specific ground motions as well as free field and non-reflecting boundaries.

- Initial conditions to dynamic analyses will include temperature from heating. Mountain-scale three-dimensional topographic thermomechanical models will be used to define the thermally induced stress state for postclosure analyses.

- Temperature input to preclosure mechanical and ground support models will be derived from NUFT ventilation and thermal analysis programs used for LA thermal analysis.

RDTME 3.15

Provide field data and analysis of rock bridges between rock joints that are treated as cohesion in DRKBA modeling together with a technical basis for how a reduction in cohesion adequately accounts for thermal effects. The DOE will provide clarification of the approach and technical basis for how reduction in cohesion adequately accounts for thermal effects, including any additional applicable supporting data and analyses. Additionally, the adequacy of the cohesion reduction approach will be verified according to the approach described in Subissue 3, Agreement 22, of the Repository Design and Thermal-Mechanical Effects Technical Exchange. This will be documented in a revision to the Drift Degradation Analysis, ANL-EBS-MD-000027, expected to be available to NRC in FY 2003.

General Approach:

- Analyses of non-lithophysal rocks will be conducted with three-dimensional discontinuum analyses.

- The fracture input to these models will be derived from simulated fracture networks developed from the FracMAN program. FracMAN will be used to develop statistically equivalent synthetic fracture networks based on field detailed line surveys and full periphery mapping in the ESF and ECRB. This method will automatically include non-penetrating fracture planes, and thus the solid rock between joints will be defined statistically.

- 3DEC parametric analyses will be used to model and test assumption of both solid rock bridges and fully penetrating fractures to determine the level of non-conservatism in assuming solid, non-failing rock bridges.

- Laboratory shear tests on simulated non-lithophysal rock bridges will be conducted by USBR as a means of calibration of numerical models of rock bridge shear strength. The PFC and UDEC programs will be used to identify impact of rock bridges on shear and tension behavior of joints. The assumed shear strength derived from these studies will be used in numerical analysis for comparison to assumed partially penetrating and fully penetrating joints.

- The level of conservatism will be documented in the revision of *Drift Degradation Analyses* (BSC 2001), to be completed in FY 2003.

RDTME 3.16

Provide a technical basis for the DOE position that the method used to model joint planes as circular discs does not under-represent the smaller trace-length fractures. The DOE will analyze the available small trace-length fracture data from the Exploratory Studies Facility and Enhanced Characterization of the Repository Block, including their effect on block development. This will be documented in a revision to the Drift Degradation Analysis, ANL-EBS-MD-000027, expected to be available to NRC in FY 2003.

General Approach:

- As discussed in RDTME 3.08, FracMAN will be used for developing fracture geometries based on 1 m and greater trace length joints. Data for FracMAN is derived from fractures data base in ESF and ECRB.

- The FracMAN approach currently provides a centroid and radius of the fracture plane. The 3DEC model that utilizes this information allows the fractures to fully penetrate the block that it cuts (i.e., conservative assumptions can be made that over-estimate the trace length of the fractures).

- Parametric studies will be conducted to examine the level of non-conservatism that arises from the assumption of fractures with disc shapes. Additionally, synthetic full-periphery structure maps will be created from the FracMAN circular disc models and compared, empirically, to actual full periphery maps to ensure the fracture patterns are geologically reasonable.

- Rockfall analyses in lithophysal rocks will determine block sizes empirically based on the density of ubiquitous, short trace length interlithophysal fracturing and the spacing of lithophysae. Density will be described in terms of fractures per cubic meter, leading to relatively small rock sizes. It will be established that the major large trace length fractures in the lithophysal rocks will not control block sizes.

- Documentation will be provided in the revision of *Drift Degradation Analyses* (BSC 2001) to be completed in FY 2003, and in *Fracture and Lithophysae Characteristics of the Repository Host Horizon* in the first quarter of FY 2004.

RDTME 3.17

Provide the technical basis for effective maximum rock size including consideration of the effect of variation of the joint dip angle. The DOE will provide the technical basis for effective maximum rock size including consideration of the effect of variation of the joint dip angle. This will be documented in revisions to Drift Degradation Analysis, ANL-EBS-MD-000027, and Rockfall on Drip Shield, CAL-EBS-ME-000001, expected to be available to NRC in FY 2003.

General Approach:

- The maximum rock size in the non-lithophysal rock will be determined directly from the 3DEC model, whose block geometry is determined from FracMAN simulated fracture networks. A large number of simulations will be conducted from probabilistically determined fracture networks that will be based on the mapped variability of fracture characteristics, including: dip and dip direction, trace length, centroid location, and spacing.

- Directional bias for dip of fractures will be accounted for in FracMAN simulations using Mauldon correction for non-persistent fractures.

- Maximum block sizes in the Tptpll will be determined empirically using observational data from the ECRB and ESF. These data will include:

  - Density of ubiquitous fractures in terms of fractures per cubic meter
  - Observations of block sizes during large diamond coring operations in ECRB

- Documentation will be provided in the revision of *Drift Degradation Analyses* (BSC 2001) to be completed in FY 2003.

RDTME 3.19

The acceptability of the process models that determine whether rockfall can be screened out from performance assessment abstractions needs to be substantiated by the DOE by doing the following: (1) provide revised DRKBA analyses using appropriate range of strength properties for rock joints from the Design Analysis

Parameters Report, accounting for their long-term degradation; (2) provide an analysis of block sizes based on the full distribution of joint trace length data from the Fracture Geometry Analysis Report for the Stratigraphic Units of the Repository Host Horizon, including small joints trace lengths; (3) verify the results of the revised DRKBA analyses using: (a) appropriate boundary conditions for thermal and seismic loading; (b) critical fracture patterns from the DRKBA Monte Carlo simulations (at least two patterns for each rock unit); (c) thermal and mechanical properties for rock blocks and joints from the Design Analysis Parameters Report; (d) long-term degradation of rock block and joint strength parameters; and (e) site-specific ground motion time histories appropriate for postclosure period; provide a detailed documentation of the analyses results; and (4) in view of the uncertainties related to the rockfall analyses and the importance of the outcome of the analyses to the performance of the repository, evaluate the impacts of rockfall in performance assessment calculations. DOE believes that Drift Degradation Analysis is consistent with current understanding of the Yucca Mountain site and the level of detail of the design to date. As understanding of the site and the design evolve, DOE will: (1) provide revised DRKBA analyses using appropriate range of strength properties for rock joints from a design parameters analysis report (or other document), accounting for their long-term degradation; (2) provide an analysis of block sizes based on the full distribution of joint trace length data from the Fracture Geometry Analysis for the Stratigraphic Units of the Repository Host Horizon, ANL-EBS-GE-000006, supplemented by available small joint trace length data; (3) verify the results of the revised DRKBA analyses using: (a appropriate boundary conditions for thermal and seismic loading; (b) critical fracture patterns from the DRKBA Monte Carlo simulations (at least two patterns for each rock unit); (c) thermal and mechanical properties for rock blocks and joints from a design parameters analysis report (or other document); (d) long-term degradation of joint strength parameters; and (e) site-specific ground motion time histories appropriate for postclosure period. This will be documented in a revision to Drift Degradation Analysis, ANL-EBS-MD-00027, expected to be available to NRC in FY 2003. Based on the results of the analyses above and subsequent drip shield calculation revisions, DOE will reconsider the screening decision for inclusion or exclusion of rockfall in performance assessment analysis. Any changes to screening decisions will be documented in analyses prior to any potential license application.

General Approach:

The keyblock approach is no longer being used as the primary method for drift degradation and rockfall analysis. Following is the revised methodology for rockfall analyses and drift degradation (details provided in Appendix B):

- 3DEC, three-dimensional discontinuum analyses (non-lithophysal rocks) will be conducted for the combination of in situ, thermal and seismic loading over the preclosure and postclosure periods.

- The 3DEC analyses will be based on fracture and block geometries defined by analysis of the detailed line surveys and full periphery mapping from the ESF and ECRB. These data will feed the FracMAN program that will be used to define statistically equivalent rock mass fracture geometries that are, in turn, used as data input to the 3DEC, three-dimensional discontinuum program that will generate the block geometries.

- Fully dynamic analyses will be used to conduct a large number of probabilistic analyses (in which fracture geometry, site-specific ground motions, joint properties and trace length characteristics are varied) to derive a probability density function of rockfall sizes and shapes.

- UDEC, two-dimensional discontinuum analyses will be used to conduct rockfall and degradation studies resulting from in situ, thermal and seismic loading in the lithophysal rocks.

- An equivalent mechanical material model, using a finely discretized UDEC block geometry will be calibrated to the range of lithophysal rock mass properties as determined from laboratory and in situ compression testing. Mechanical properties will be directly related to lithophysal porosity and its variability. Model will allow rock mass failure, fracturing and rockfall.

- Parametric studies will be conducted for the full range of variability of the lithophysal rock mass properties.

- Site-specific ground motions will be applied to the models, based on hazard curves derived from *Probabilistic Seismic Hazard Analyses for Fault Displacement and Vibratory Ground Motion at Yucca Mountain, Nevada* (CRWMS M&O 1998).

- These studies will provide rock size, shape and velocity to analyses of the drip shield as a function of time.

All of this work will be documented in the revision of *Drift Degradation Analyses* (BSC 2001), to be completed in FY 2003.

A.2 REFERENCES

A.2.1. DOCUMENTS CITED

BSC (Bechtel SAIC Company, LLC) 2001. *Drift Degradation Analysis*. ANL-EBS-MD-000027 REV 01 ICN 01. Las Vegas, Nevada: Bechtel SAIC Company. ACC: MOL.20011029.0311.

CRWMS M&O (Civilian Radioactive Waste Management System Managing and Operating Contractor) 1998. *Probabilistic Seismic Hazard Analyses for Fault Displacement and Vibratory Ground Motion at Yucca Mountain, Nevada*. Milestone SP32IM3, September 23, 1998. Three volumes. Las Vegas, Nevada: CRWMS M&O. ACC: MOL.19981207.0393.

APPENDIX B

THERMAL AND MECHANICAL ROCK PROPERTIES DATA BASE

INTENTIONALLY LEFT BLANK

APPENDIX B: THERMAL AND MECHANICAL ROCK PROPERTIES DATA BASE

B.1   LABORATORY PROPERTIES DATA BASE

Over the past 22+ years a vast amount of data has been collected on the mechanical properties of the intact rock within Yucca Mountain, Nevada (Table B-1, Table B-2, and Table B-3). All of the studies were performed under the existing guidelines at the time, and, therefore, not all of the data were gathered under a qualified QA program (Table B-1). No matter what the pedigree of the data, we can, however, gain much insight from all of the data.

B.1.1   MECHANICAL DATA

In the late 1970's and through the mid-1980's, many samples were tested from units extending from the upper-most parts of the Paintbrush Tuff down through the lower regions of the Crater Flat Tuff. From the beginning, an approach was adopted to assign a baseline set of conditions and then study the effects of all other conditions (i.e., sample related, environmental and inherent rock characteristics) relative to that standard. Initially, samples were difficult to obtain, so the baseline conditions were defined as: each test specimen was machined as a right-circular-cylinder, with a nominal diameter of 25 mm (1 in.) and a 2:1 length:diameter ratio, and tested in a water-saturated state at room temperature, atmospheric pressure, and a nominal axial strain rate of 10^{-5} s^{-1}. The results from these test series (Olsson and Jones 1980; Nimick et al. 1985; Price and Jones 1982; Price, Jones, and Nimick 1982; Price and Nimick 1982; Price, Nimick and Zirzow 1982; Price, Spence, and Jones 1984) revealed that there is some lateral (i.e., within a unit) and vertical (i.e., unit to unit) variability. However, the variabilities in the elastic and strength properties of the tuffs (all having similar chemical constituents) are predominantly a function of the tuff porosity (Figure B-1, Price 1983 and Price and Bauer 1985). In addition, while it is not a significant factor within the Topopah Spring Member tuffs, in a broader sense the relationships were found to be stronger when the properties were fit to functional porosity–defined as pore space plus the volume fraction of montmorillonite, a very low strength clay mineral (Price and Bauer 1985) illustrates this relationship. In addition, some of the data also helped in the early understanding of the effects of changes in saturation, temperature, pressure, and rate (Price 1983).

Beginning in the mid-1980's, effort was concentrated on the Topopah Spring Member tuff, and specifically on the unit referred to today as the middle Tptpmn, which was considered at that time to be the target horizon for the potential repository. Because of the larger inhomogeneities in the welded tuffs of the Topopah Spring Member, the size of the baseline samples was increased to nominally 51 mm (2 in.) in diameter. The remainder of the baseline conditions remained the same. The studies also began to incorporate some detailed information on the petrology and pore distribution of both the lithophysal and nonlithophysal zones (Price et al. 1985 and Price, Connolly, and Keil 1987, respectively). These studies determined that the most predominant secondary factor in the scatter of the plots of strength or Young's modulus vs. porosity is the distribution of the porosity. In Busted Butte samples of the middle nonlithophysal zone, the vast majority of pores were found to be intergranular openings (usually less than 5 μm across) (Price, Connolly and Keil 1987). In general for the welded tuffs, a study on Busted Butte samples of the upper lithophysal zone found that there are four size classes of pores (Figure B-2). They are: large   lithophysal   cavities   (few   millimeters   on   up),   small   pores   in   the

vapor-phased-altered zones (up to 0.2 mm), intergranular pores in vapor-phased-altered zones (in the range of 1-5 μm, and 0.2 mm), intergranular pores in vapor-phased-altered zones (in the range of 1-5 μm), and submicroscopic intergranular pores in the devitrified matrix (smaller than 1 μm) (Price et al. 1985).

The next key study (Price 1986) examined the effect of sample size on the elastic and strength properties of the middle nonlithophysal zone of the Topopah Spring tuff (Figure B-3). Sometime later a model relating strength, sample size and functional porosity was developed (Price 1993) from these data in combination with the early fits of strength vs. functional porosity.
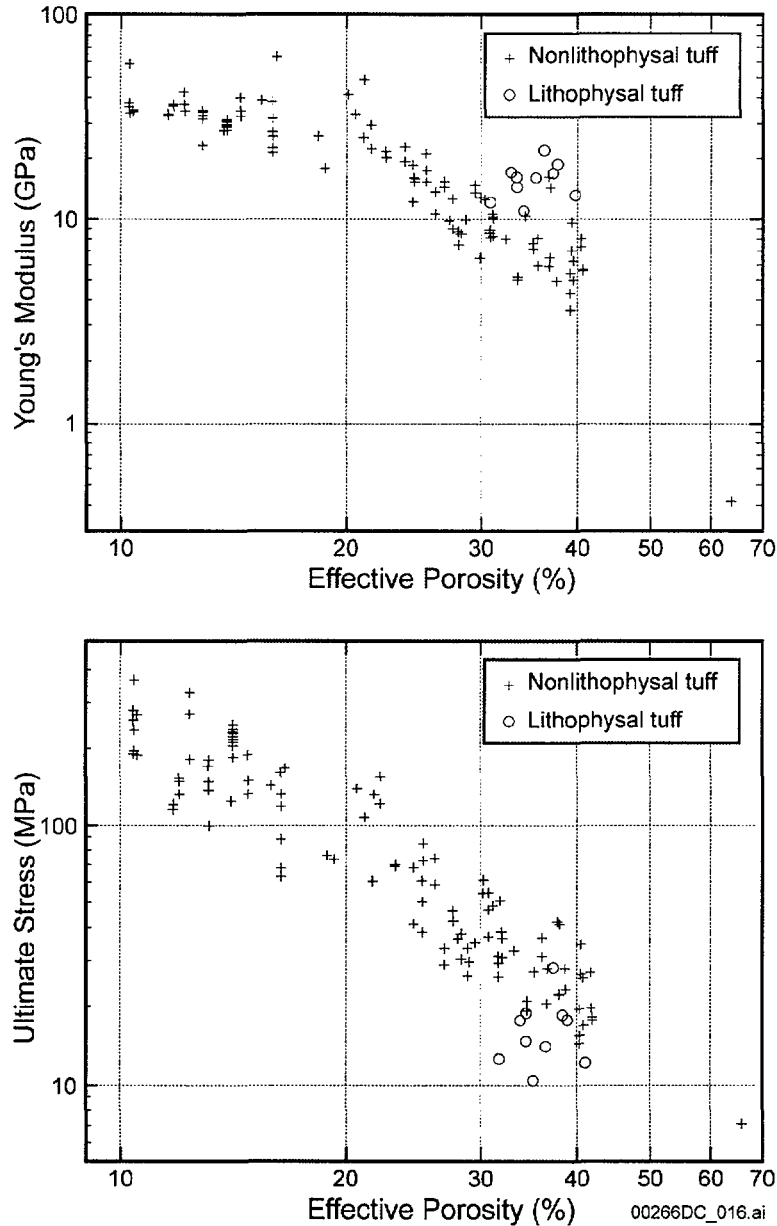
Source: Price et al. 1985.

Figure B-1. Intact Rock Modulus and Strength as a Function of Effective Porosity
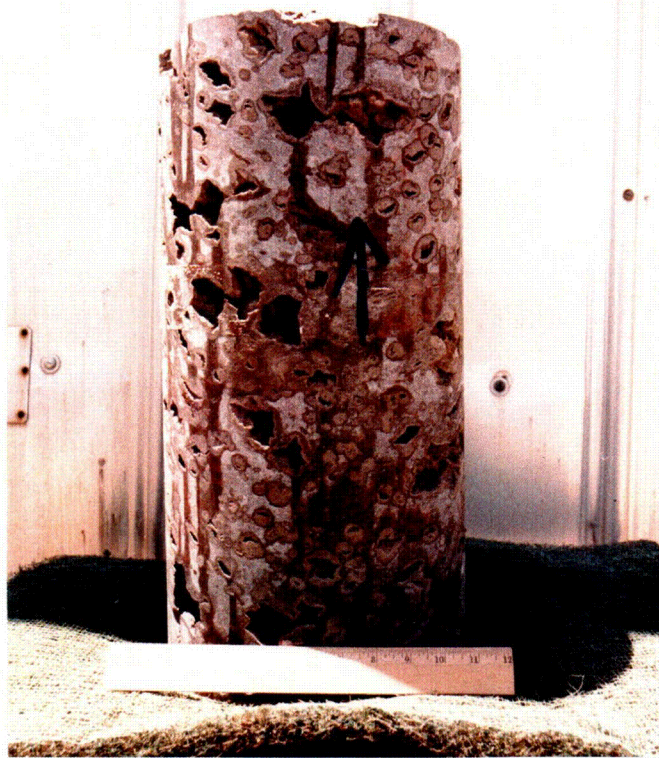
00266DC_018 Pt 2.ai

Source: Price et al. 1985.

Figure B-2. Photograph of Busted Butte Sample from the Upper Lithophysal Zone (Tptpul)

During the early to mid-1990's, techniques were formalized (e.g., Boyd, Martin and Price 1994; Martin et al. 1991; Price, Martin and Haupt 1994) and data were collected under a qualified QA program. Most of the data from this period of time were published in a series of data reports (Boyd, Martin, and Price 1995; Boyd et al. 1996a and 1996b; Martin et al. 1994 and 1995; Martin, Noel, Boyd, and Price 1997a). In addition to the standard reporting of elastic and strength properties, these reports present detailed bulk properties (e.g., average grain density, bulk density, porosity), compression- and shear-wave velocity measurements, and CT (computerized tomography) scans on the samples. Analyses (Price et al. 1994 and 1996) showed that the relationships between elastic and strength properties vs. porosity were very similar for these data on larger samples (with the baseline diameter of 51 mm) to those found earlier on the smaller samples (with the baseline diameter of 25 mm). The only significant change was a shift downward (i.e., lower) in the strength data, which would be expected because of the larger sample size (Figure B-4).

During this same time span, some studies have focused on the inherent mechanical property characteristics, as well as the effects of changes in many environmental conditions on the mechanical properties of the intact tuffs. For example, many data have been collected showing that the anisotropy in velocity measurements is almost universally less than 10 percent. The results of a specific study on this effect revealed a velocity anisotropy of about 7 percent (Martin

C09

et al. 1992), which is a relatively minor effect with respect to the natural scatter in the tuff data, in general.

The attenuation properties of the nonlithophysal tuffs were also examined (Haupt et al. 1992; Price, Martin and Haupt 1994). Extensional attenuation was found to be virtually unaffected by frequency (for dry samples) or strain amplitude changes (for both dry and saturated samples). However, attenuation did increase with increasing frequency for the saturated samples.
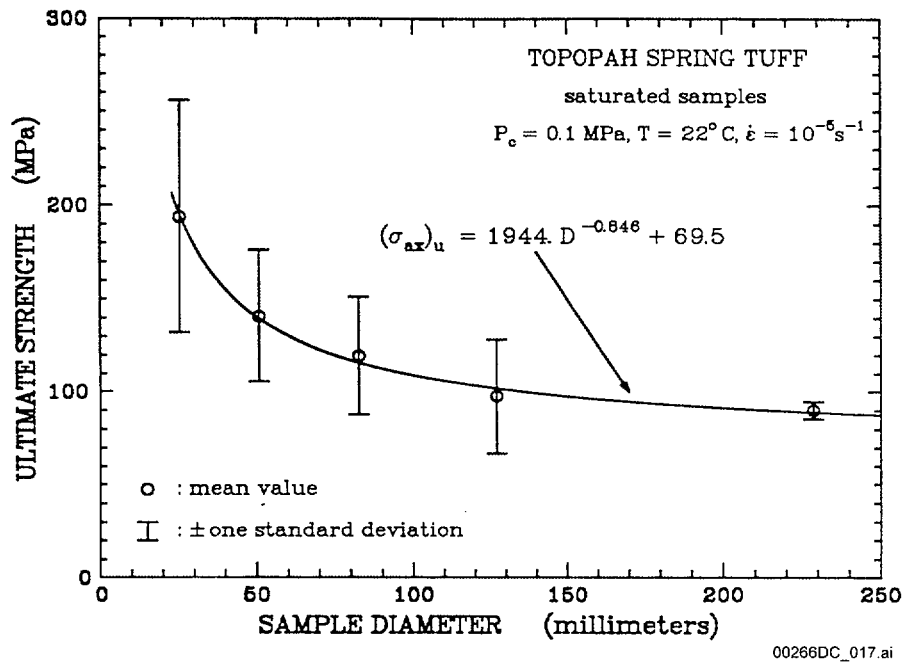
The collecting of CT scans has provided information in addition to that collected in the mid-1980's for the study on the distribution of porosity within the Topopah Spring tuffs. An initial analysis (Price, Martin and Boyd 1993) relating qualities observed on the CT scans to the Young's modulus and ultimate strength of nonlithophysal tuff samples produced good correlations.

Many studies have shown strong relationships between static Young's modulus and effective porosity and ultimate strength and effective porosity. In order to investigate whether the dynamic properties showed the same types of relationships or not, the results from a series of samples were analyzed (Price et al. 1994). Initially, velocity measurements were taken, dynamic Young's moduli were calculated, and then the samples were tested at the baseline set of conditions. Both the P-wave velocities and the dynamic Young's moduli showed similar correlation with porosity, as do the static Young's moduli. Furthermore, in a direct comparison of the static and dynamic Young's moduli, the dynamic moduli are consistently higher in value than the static moduli. This result was not surprising, because this is the normal relationship between static and dynamic moduli for brittle materials.

Several studies (Martin et al. 1993a, 1993b, 1995; Martin, Noel, Boyd, and Price 1997b and 1997c) have produced indications that the strength properties of the tuffs are somewhat time dependent. Except at very fast rates of deformation (i.e., an axial strain rate of 10^{-3} s^{-1}), the strengths of the tuffs were found to decrease with decreasing strain rate (from 10^{-5} s^{-1} to 10^{-9} s^{-1}), although the average change was relatively minor (about a 10 percent decrease in strength per decade change in strain rate). In addition, constant stress (creep) experiments at fairly high stresses (most tests at 100 MPa and higher) resulted in very little strain accumulating after several million seconds. In one study on Topopah Spring tuffs from Busted Butte (having an average quasi-static, unconfined compression strength of nearly 150 MPa), the fit of the data from static fatigue tests predicts that under a constant load of 100 MPa, the rock would fail in 7.1×10^9 years.

In summary, a large amount of data has been collected to date on tuffaceous samples from Yucca Mountain at a baseline set of conditions. These data have shown that the variabilities in elastic and strength properties are not a function of lateral or vertical position, but primarily a function of porosity. In stratigraphic zones that contain montmorillonite (a very weak clay material), the fits are improved by adding the volume of this mineral to the porosity and calling this quantity functional porosity. Even though there are excellent trends in the Young's modulus, strength, and compression velocity data when plotted against porosity, the data has a significant scatter to it. The secondary effect that is creating the scatter is the distribution of the porosity. Other investigations have examined the effects of many other conditions (i.e., sample related, environmental and inherent rock characteristics); for example, sample size, saturation, pressure,

temperature, deformation rate, attenuation, anisotropy have all been studied. In conclusion, the intact rock mechanical property information collected over the last two decades has provided a good understanding of many aspects of the behavior of Yucca Mountain tuffs. However, the data set available for licensing type activities would be more complete with the collection of some additional data on several issues within the requirements of a qualified QA program. A few of the major issues needing additional data include studying the effects of lithophysal cavities, sample size, and constant stress loading.

TOPOPAH SPRING TUFF

saturated samples

$P_c = 0.1\ \text{MPa},\ T = 22^\circ C,\ \dot{\varepsilon} = 10^{-5}\text{s}^{-1}$

$(\sigma_{ax})_u = 1944.\ D^{-0.846} + 69.5$

o : mean value

$\perp$: ± one standard deviation

00266DC_017.ai

Source: Price 1986.

Figure B-3. Effect of Sample Size on the Uniaxial Compressive Strength of Welded Tuff from the Middle Nonlithophysal Zone (Tptpmn)

(a)

NRG Data

$E = 85.5\, e^{-6.96\, n}$

$E = 74.3\, e^{-8.60\, \phi}$

Youngs Modulus (GPa)

Porosity

(b)

NRG Data

$\sigma_u = 4.04\, n^{-1.85}$

$\sigma_u = 0.946\, \phi^{-2.14}$

Ultimate Strength (MPa)

Porosity

(c)

NRG Data

$T_0 = 20.2\, e^{-8.39\, o}$

Tensile Strength (MPa)

Porosity

00266DC_050.ai
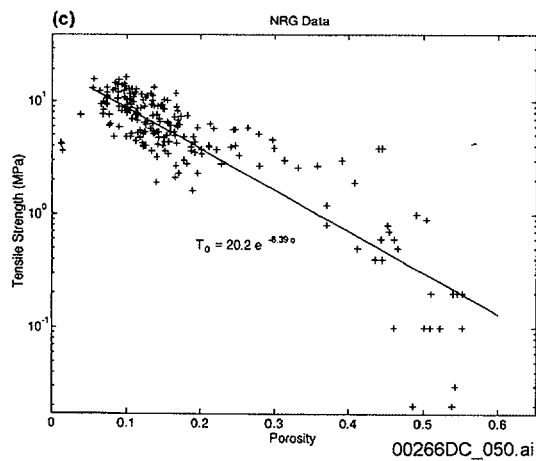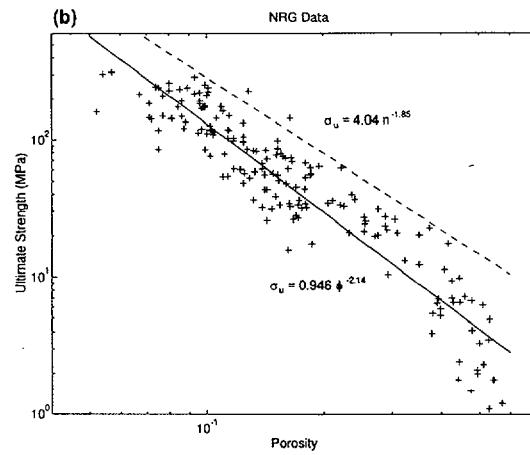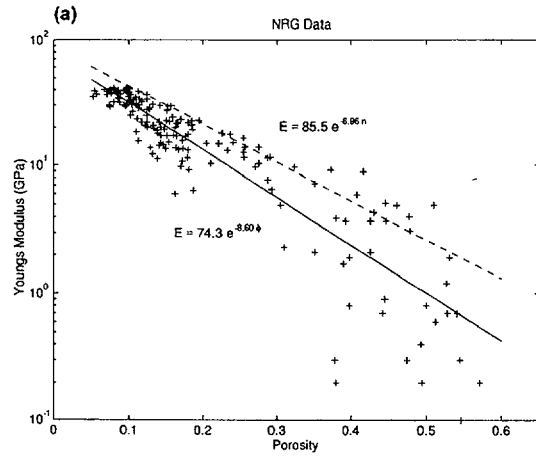
Source: Price et al. 1996.

Figure B-4. Modulus (a), Compressive Strength (b), and Tensile Strength (c) as Functions of Porosity

B.1.2 THERMAL DATA

A significant amount of thermal properties data have also been collected since the early 1980's. Primary parameters of interest are thermal conductivity, thermal capacity, and thermal expansion. Thermal properties are largely a function of mineralogy, and so a phenomenological understanding of these properties requires that mineralogy be determined. The most complete data sets of thermal properties data from the repository horizon as well as units above and below were developed from specimens taken from four boreholes drilled along the North Ramp of the Exploratory Studies Facility (boreholes UE25 NRG-4, UE25 NRG-5, USW NRG-6, and USW NRG-7/7A). A total of 143 thermal conductivity tests, 132 thermal expansion tests, and 10 specific heat tests were conducted from specimens taken from various horizons in theses boreholes. Thermal expansion and thermal conductivity tests were also performed on test specimens taken from Alcoves 5 and 7 within the Exploratory Studies Facility (ESF). In these tests, specimens were oriented orthogonally and so anisotropy as well as lateral variability of thermal properties could be measured. Results from all thermal tests show very limited evidence of lateral variability and anisotropy within each tuff unit.

Standard test conditions for thermal conductivity measurements included four saturation levels: vacuum saturated, partially saturated, air-dried (no effort was made to preserve or alter the moisture content), and oven-dried. Thermal expansion test specimens were either air-dried, oven-dried, or vacuum saturated. All specific heat measurements were made on air-dried specimens. Tests were conducted at room pressure and at temperatures between 25°C and 300°C. Because many specimens were tested at multiple saturation states, there are more tests than test specimens. Thermal conductivity, thermal expansion, specific heat, and X-ray diffraction measurement methods are discussed in detail in Brodsky et al. 1997. The thermal properties measurements were made by the Testing Services Division of Holometrix, Inc. and the X-ray diffraction measurements were conducted at the University of New Mexico.

The thermal conductivity data from the NRG boreholes are summarized in Table B-1. Data are consistent with previous values reported in Nimick (1989) which includes both published and previously unpublished results. Thermal conductivities measured on saturated specimens exceeded those measured on dried specimens. For dried specimens, conductivity is essentially constant with increasing temperature. For saturated specimens, conductivities sometimes increased and sometimes decreased with increasing temperature. Decreases in thermal conductivity in specimens containing moisture may be affected by specimen dehydration. There were no consistent differences in thermal conductivities among the boreholes and so the data were averaged together. PTn consistently shows the lowest conductivities while the TCw and TSw2 units have the highest conductivity values. TSw1 specimens span a larger range of thermal conductivity and are intermediate in value. These data show that there is no substantial temperature dependence.

Thermal/ Mechanical Unit	Thermal Conductivity (W/mK)											
	Saturated			Partially Saturated			Air Dry			Dry		
	Sample Mean	Sample Standard Deviation	Sample Count	Sample Mean	Sample Standard Deviation	Sample Count	Sample Mean	Sample Standard Deviation	Sample Count	Sample Mean	Sample Standard Deviation	Sample Count
TCw	1.89	0.12	18	1.39	0.56	18	1.58	0.16	9	1.17	0.35	18
PTn	0.92	0.13	42	0.57	0.12	33	0.35	0.13	12	0.38	0.10	49
TSw1	1.70	0.19	50	1.23	0.46	11	1.21	0.12	30	0.98	0.26	59
TSw2	2.29	0.42	51	ND	ND	ND	1.66	0.10	24	1.50	0.44	48

[a] ND: No Data. "Sample" refers to the number of test measurements, not the number of specimens tested. Measurements were made during both heating and cooling for some specimens.

Table B-2. High Temperature (>100°C) Rock Thermal Conductivities [a]

Thermal/ Mechanical Unit	Thermal Conductivity (W/mK)		
	Dry		
	Sample Mean	Sample Standard Deviation	Sample Count
TCw	1.53	0.17	57
PTn	0.42	0.14	102
TSw1	1.15	0.15	173
TSw2	1.59	0.10	125

"Sample" refers to the number of test measurements, not the number of specimens tested. Measurements were made during both heating and cooling for some specimens.

Attempts have been made to correlate thermal conductivity with an easily measured physical property such as porosity. Figure B-5 shows thermal conductivities obtained at 30°C on oven dry specimens plotted vs. porosity. Both the Woodside and Messmer (1961) and the Brailsford and Major (1964) equations, which predict this relationship, are shown. The models were fitted to the data as follows. Based on the measured saturation and porosity of each specimen, the matrix conductivity (i.e., conductivity at zero porosity) for each specimen was calculated for each model. These matrix conductivities were then averaged for each model to obtain the conductivity at zero porosity. The change in conductivity with increasing porosity was then calculated directly from each model. Unfortunately, lithologies also change with increasing porosity and so it is difficult to isolate the effects of changing one variable. The TSw2 data appear to cluster into three groups. The high and low thermal conductivity groups are both from NRG-5 and include the Tptpmn lithostratigraphic unit (Buesh et al. 1996). The intermediate thermal conductivity group is from NRG-6 and includes both the Tptpmn and Tptpln lithostratigraphic units.

The mean coefficients of thermal expansion (MCTE) are summarized in Table B-3 for heating. Similar data exist for the cooling cycles. Within each table, the information is grouped according to T/M unit and moisture content.
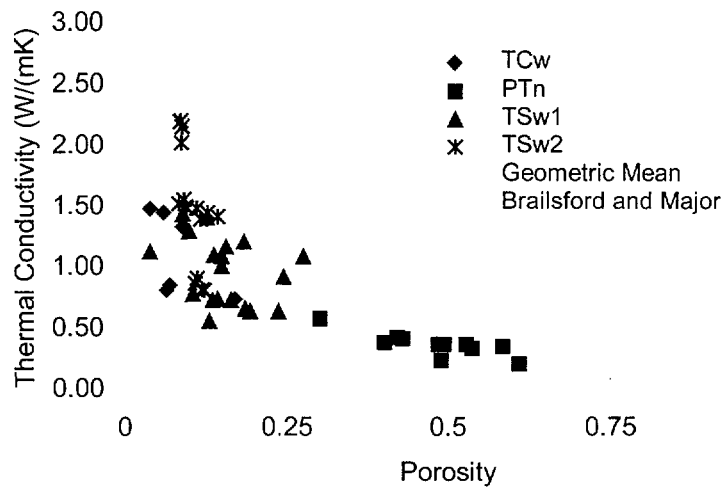
Figure B-5. Thermal Conductivity vs. Porosity for Oven-Dried Specimens from NRG Boreholes

As shown in Table B-3, MCTEs are highly temperature dependent. The strains increase (expansion is positive) for both tuffs until a "transition temperature" of approximately 150° to 225°C is reached. In both cases, the strain-versus-temperature curves then become more highly nonlinear; however, the slope increases for the welded specimen while it decreases for the nonwelded specimen. For the welded specimens, thermal expansion was independent of saturation state; however, thermal strains did depend upon saturation for the nonwelded rocks (Brodsky et al. 1997).

The increase in thermal strains between 150°C and 225°C (the "transition temperature" range) observed for many of the welded devitrified specimens is likely to be due to phase transitions in the constituent minerals of tridymite and cristobalite. These minerals occur, with or without quartz, as primary devitrification products in many samples of Yucca Mountain welded tuffs. Phase transitions in synthetic tridymite occur at approximately 117°C and 163°C, and in synthetic cristobalite at approximately 272°C (Papike and Cameron 1976), and involve notable changes in volume. Phase transition temperatures have been shown to vary significantly due to lattice variations found in natural occurrences of these minerals which are usually mixed phase material (Thompson and Wennemer 1979). Previous and current work on the mineralogy of welded tuff from TCw, TSw1, TSw2, and TSw3 suggest that these mixed phase assemblages are dominant. Hysteresis is associated with the phase changes because the phases invert at higher temperature during heating than during cooling. The irreversible expansion may be a consequence of incomplete phase inversion on cooling.

For the nonwelded specimens, some of the strain decrease (near 100°C) is attributable to loss of pore water, but most of the irreversible strain is probably a consequence of dehydration of perlitic volcanic glass and clay minerals at elevated temperatures which results in a permanent volume decrease.

Some specimens that displayed sensitivity to transition temperature were analyzed to assess the role of the maximum test temperature. Specimens from approximately the same depth (i.e., from the same piece of original core) were tested to different temperatures. The results showed that as

long as the maximum test temperature remained below the transition temperature, the specimens did not permanently change dimension (i.e., no hysteresis was evident). The specimens expanded during the heating phase along a nearly linear curve and contracted during cooling along the same curve, with no discontinuity. These tests indicated that the transition temperatures probably caused physical changes in tuff that altered the expansion characteristics. The maximum temperature to which the specimens were exposed affected the magnitude of the hysteresis in the strain-versus-temperature curves.

Table B-3. Mean Coefficient of Thermal Expansion During Heat-Up

Saturation State	Statistics[a]	Mean CTE on Heat-up ($10^{-6}/^{\circ}$C)										
		25-50°C	50-75°C	75-100°C	100-125°C	125-150°C	150-175°C	175-200°C	200-225°C	225-250°C	250-275°C	275-300°C
Saturated	Mean	7.09	7.62	8.08	10.34	13.17	15.20	16.99	18.99	21.38	27.42	42.99
	Std. Dev.	0.43	0.15	0.50	1.52	1.23	1.57	1.41	0.96	1.23	1.94	37.35
	Count	4	4	4	4	4	4	4	3	3	3	3
Dry	Mean	6.60	8.29	9.62	10.53	12.69	14.90	17.03	20.68	29.64	36.49	49.15
	Std. Dev.	1.49	0.99	1.06	1.60	1.55	1.91	2.31	5.41	21.88	16.97	34.24
	Count	10	10	10	7	7	7	7	7	7	7	7
		25-50°C	50-75°C	75-100°C	100-125°C	125-150°C	150-175°C	175-200°C	200-225°C	225-250°C	250-275°C	275-300°C
Saturated	Mean	4.46	4.28	-1.45	-30.42	5.54	4.47	0.64	-4.65	-9.79	-13.46	-12.96
	Std. Dev.	0.38	1.61	3.63	21.47	0.41	0.79	1.03	4.05	7.85	11.12	12.90
	Count	4	4	4	4	3	3	3	2	2	2	2
Dry	Mean	4.55	4.24	3.36	-4.78	6.46	5.69	3.61	0.56	-2.98	-5.81	-7.25
	Std. Dev.	0.74	1.46	2.40	11.12	0.98	1.41	2.58	5.81	9.12	11.36	10.80
	Count	12	12	12	10	10	10	10	10	10	10	10
		25-50°C	50-75°C	75-100°C	100-125°C	125-150°C	150-175°C	175-200°C	200-225°C	225-250°C	250-275°C	275-300°C
Saturated	Mean	6.56	7.32	6.83	6.92	10.72	14.28	20.98	36.82	41.64	42.76	43.81
	Std. Dev.	1.16	0.60	1.60	3.28	1.74	3.26	7.01	20.49	17.35	13.19	13.65
	Count	10	10	10	10	10	9	9	8	8	8	8
Dry	Mean	6.29	7.60	8.39	8.96	10.37	15.51	23.67	34.24	34.00	36.07	38.74
	Std. Dev.	1.22	1.02	0.89	1.20	1.38	4.53	11.07	20.30	13.70	13.23	13.78
	Count	33	33	33	28	28	27	26	25	25	25	25
		25-50°C	50-75°C	75-100°C	100-125°C	125-150°C	150-175°C	175-200°C	200-225°C	225-250°C	250-275°C	275-300°C
Saturated	Mean	7.14	7.47	7.46	9.07	9.98	11.74	13.09	15.47	19.03	25.28	37.19
	Std. Dev.	0.65	1.51	1.21	2.41	0.77	1.28	1.40	1.75	3.09	6.87	14.27
	Count	19	19	19	19	19	19	19	16	16	16	16
Dry	Mean	6.67	8.31	8.87	9.37	10.10	10.96	12.22	14.52	20.79	25.13	35.13
	Std. Dev.	1.20	0.42	0.40	0.55	0.88	1.16	1.50	2.57	17.03	10.07	14.56
	Count	40	40	40	40	40	38	38	35	35	35	35

[a] Std. Dev. = standard deviation.

All of the thermal expansion data presented in Table 4-3 were obtained at ambient pressure. Mineralogical phase changes are pressure sensitive and the temperatures at which these transitions occur increase with pressure. Additionally, pressure will suppress volume expansion within fractures and voids. A suite of confined thermal expansion tests was therefore conducted to determine if strain hysteresis and transition temperature effects would be suppressed by elevated pressures. These tests are discussed in detail in *Thermal Expansion of the Paintbrush Tuff Recovered from Borehole USW SD-12 at Pressures 30 MPa: Data Report* (Martin et al. 1997). This report concluded that pressure effects for specimens tested between 1 and 30 MPa were very small, so data from these pressures were averaged together.

Thermal capacitance data from the NRG boreholes are summarized in Table B-4. Thermal capacitance is higher for TSw2 than for TSw1. All specimens show a localized peak in thermal capacitance at 150°C - 170°C. In general, thermal capacitance increases monotonically until this temperature range is reached. For all TSw1 specimens and some TSw2 specimens, thermal capacitance then decreases slightly with increasing. Above 150°C - 170°C, other TSw2 specimens show initial decreases in thermal capacitance followed by nearly constant values.

Table B-4. Thermal Capacitance ($\rho \cdot Cp$) of Topopah Spring Tuff

TSw1				TSw2			
Temperature (°C)	Mean $\rho \cdot Cp$ (J·cm^{-3}·K^{-1})	Standard Deviation (J·cm^{-3}·K^{-1})	No. of Tests	Temperature (°C)	Mean $\rho \cdot Cp$ (J·cm^{-3}·K^{-1})	Standard Deviation (J·cm^{-3}·K^{-1})	No. of Tests
25	1.58	0.05	3	25	1.79	0.11	7
50	1.68	0.05	3	50	1.88	0.11	7
75	1.80	0.05	3	75	1.97	0.11	7
100	1.91	0.05	3	100	2.16	0.11	7
125	2.03	0.06	3	125	2.32	0.11	7
150	2.14	0.11	3	150	2.45	0.13	7
175	2.13	0.10	3	175	2.43	0.18	7
200	2.09	0.07	3	200	2.40	0.16	7
225	2.07	0.06	3	225	2.39	0.17	7
250	2.05	0.05	3	250	2.39	0.19	7
275	2.03	0.05	3	275	2.39	0.22	7
300	2.03	0.06	3	300	2.43	0.26	7

It is believed that the peaks in specific heat shown in Table B-4 are related to phase changes; however, the data presented here are insufficient to correlate these peaks more specifically with mineralogy. It is worth noting that the peaks in specific heat at 150°C - 170°C occur at a temperature range associated with the phase change in tridymite (163°C). It is also evident that there were no significant changes in specific heat for these air-dried specimens at 100°C, indicating that dehydration effects were minor.

Values of thermal capacitance were calculated by Nimick and Connolly (1991) from chemical and mineralogical data and published heat capacity data for the constituent minerals. For both the theoretical and experimental data, values for TSw2 are higher than for TSw1. The two sets of data roughly coincide, which is very encouraging considering that there were many

assumptions inherent in Nimick and Connolly's work. Measurements of specific heat are very sensitive to moisture content and to the types of water present. The experimental data were obtained on air-dried specimens containing 0.3 percent to 0.7 percent water by weight, whereas the calculated data were based on a water content of 5.5 percent by weight. Additionally, Nimick and Connolly (1991) believed that calculated values above 100°C would probably be high because they assumed that all H_2O^+ remained in the glass during heating. Calculated values near 100°C were omitted from the plot because they were highly influenced by heat of vaporization of water.

Mineralogies were examined to determine if correlations exist between thermal properties and the presence of certain minerals. Thermal conductivity data did not indicate any dependence on apparent mineral phase changes. The thermal expansion test results showed temperatures over which MCTEs increased steeply and hysteresis was observed. These characteristics of the thermal expansion curves were discussed in light of phase changes expected in tridymite and cristobalite.

In summary, a very extensive data set for thermal conductivity and thermal expansion exists, primarily from boreholes UE25 NRG-5, UE25 NRG-5, USW NRG-6, and USW NRG-7/7A; but supplemented by data from Alcoves 5 and 7. For the NRG test series, a total of 143 thermal conductivity tests were conducted on 95 test specimens, 132 thermal expansion tests were conducted on 120 specimens, and 10 specific heat tests were conducted on 10 specimens. Specimens were tested at several saturation states, at room pressure, and at temperatures up to 300°C. Petrologic data were obtained from 97 NRG-6 samples.

Thermal conductivities are highest for saturated specimens and lowest for dried specimens. Thermal conductivities, averaged over all boreholes, ranged (depending upon temperature and saturation state) from 1.2 W/m°K to 1.9 W/m°K for TCw, from 0.4 W/m°K to 0.9 W/m°K for PTn, from 1.0 W/m°K to 1.7 W/m°K for TSw1, and from 1.5 W/m°K to 2.3 W/m°K for TSw2. Thermal conductivity results showed that for oven dried specimens, thermal conductivities increased slightly or remained constant as temperature increased from 25°C to 300°C. The PTn T/M unit consistently showed the lowest thermal conductivities while the TCw and TSw2 units had the highest conductivity values. TSw1 specimens spanned a large range of thermal conductivities and were intermediate in value.

Mean coefficients of thermal expansion were highly temperature dependent and values, averaged over all boreholes, range (depending upon temperature and saturation state) from 6.6×10^{-6}°C^{-1} to 49×10^{-6}°C^{-1} for TCw, from the negative range to 16×10^{-6} °C^{-1} for PTn, from 6.3×10^{-6}°C^{-1} to 44×10^{-6}°C^{-1} for TSw1, and from 6.7×10^{-6}°C^{-1} to 37×10^{-6}°C^{-1} for TSw2. Thermal expansion coefficients showed substantive differences between welded and nonwelded specimens. Moisture effects were apparent in nonwelded specimens. Even for oven dried specimens, the nonwelded PTn T/M unit showed dehydration and volume loss at 100°C. At more elevated temperatures, these specimens generally continued to shorten as bound water was released. Thermal expansion of the welded specimens showed no moisture dependence. At temperatures near 200°C, hysteresis in the strain-versus-temperature curves became apparent in most specimens. Most of this was probably caused by phase changes in tridymite and cristobalite; however, this was not clear from comparison of thermal expansion and

mineralogical data. Although most expansion reversed during cooling, substantial permanent elongations (up to 200 microns or 0.4 percent strain) were observed.

Thermal capacitance values are lower for TSw1 specimens from NRG-4 than for TSw2 specimens from NRG5. Mean values of thermal capacitance (averaged over all specimens) ranged from 1.6 $J \cdot cm^{-3} \cdot K^{-1}$ to 2.1 $J \cdot cm^{-3} \cdot K^{-1}$ for TSw1 and from 1.8 $J \cdot cm^{-3} \cdot K^{-1}$ to 2.5 $J \cdot cm^{-3} \cdot K^{-1}$ for TSw2. The irregular slopes of the specific heat-versus-temperature curves are most likely related to phase changes. No mineralogical data were obtained for NRG-4 and NRG-5 specimens.

There is very little evidence of lateral variability of thermal properties within units. There is also very little data to suggest thermal properties show any degree of anisotropy (vertical vs. horizontal).

B.2   IN SITU THERMAL AND MECHANICAL PROPERTIES

The Yucca Mountain Project has supported collection of information on in situ thermomechanical properties since the mid-1990's. In situ thermal conductivity, thermal expansion, and rock mass modulus were estimated in the Single Heater Test and in the Drift Scale Test. From the Single Heater Test, the rock mass thermal expansion was estimated from displacement and temperature measurements to be between $2.5 \times 10^{-6}/°C$ to $6 \times 10^{-6}/°C$ for temperatures up to about 160°C (DTN: SNF35110695001.009), although analyses of the test suggest that intact thermal expansion coefficients provide a better match to the overall measured displacements and temperatures. Likewise, the thermal conductivity (of matrix materials) derived from back-fitting in situ data and numerical modeling suggest thermal conductivities of 2.1 W/(m·K) for wet and 1.67 W/(m·K) for dry conditions respectively (DTN: SNF35110695001.009). For rock mass modulus, the Plate Loading Test conducted as part of the larger Drift-Scale Test estimated rock mass modulus from 11.4 GPa to 29.5 GPa for ambient and thermally perturbed fractured tuffs in the vicinity of the Drift-Scale Test (George et al. 1999). A later test conducted in the same location showed higher general modulus recommended values ranging from 17.3 GPa to 43 GPa (Williams 2001). It is also possible to garner information about the rock mass strength by estimation of the stresses surrounding the Drift-Scale Test, and by estimating the strength to be some value greater than the estimated stress (by virtue of no known major rock mass failures surrounding the Drift-Scale Test).

B.3   REFERENCES

B.3.1. DOCUMENTS CITED

Boyd, P.J.; Martin, R.J., III; and Price, R.H. 1994. *An Experimental Comparison of Laboratory Techniques in Determining Bulk Properties of Tuffaceous Rocks*. SAND92-0119. Albuquerque, New Mexico: Sandia National Laboratories. ACC: NNA.19940315.0003.

Boyd, P.J.; Price, R.H.; Martin, R.J.; and Noel, J.S. 1996. *Bulk and Mechanical Properties of the Paintbrush Tuff Recovered from Boreholes UE25 NRG-2, 2A, 2B, and 3: Data Report*. SAND94-1902. Albuquerque, New Mexico: Sandia National Laboratories. ACC: MOL.19970102.0002.

Boyd, P.J.; Price, R.H.; Noel, J.S.; and Martin, R.J. 1996. *Bulk and Mechanical Properties of the Paintbrush Tuff Recovered from Boreholes UE25 NRG-4 and -5: Data Report.* SAND94-2138. Albuquerque, New Mexico: Sandia National Laboratories. ACC: MOL.19970102.0004.

Brailsford, A.D. and Major, K.G. 1964. "The Thermal Conductivity of Aggregates of Several Phases, Including Porous Materials." *British Journal of Applied Physics, 15,* 313-319. London, England: Institute of Physics. TIC: 223876.

Brodsky, N.S.; Riggins, M.; Connolly, J.; and Ricci, P. 1997. *Thermal Expansion, Thermal Conductivity, and Heat Capacity Measurements for Boreholes UE25 NRG-4, UE25 NRG-5, USW NRG-6, and USW NRG-7/7A.* SAND95-1955. Albuquerque, New Mexico: Sandia National Laboratories. ACC: MOL.19980311.0316.

George, J.T., Finley, R.E., and Riggins, M. 1999. "Conduct of Plate Loading Tests at Yucca Mountain, Nevada." *37th U.S. Rock Mechanics Symposium, Vail Colorado, June 6-9.* pp. 721-727. Vail, Colorado: American Rock Mechanics Association. TIC: 245246.

Haupt, R.W., Martin, R.J., Price, R.H., Dupree, W.J., and Tang, X. 1992. "Modulus Dispersion and Attenuation in Tuff and Granite." *33rd US Rock Mechanics Symposium, Santa Fe, New Mexico.* pp. 899-908. Rotterdam, Netherlands: American Rock Mechanics Association. TIC: 212624.

Martin, R.J., Boyd P.J., Noel J.S., and Price R.H. 1991. *Procedure Development Study: Low Strain Rate and Creep Experiments.* SAND91-0527. Albuquerque, NM: Sandia National Laboratory. ACC: NNA.19911010.0047.

Martin, R.J., Noel, J.S., Boyd, P.J., and Price, R.H. 1997a. *The Effects of Confining Pressure on the Strength and Elastic Properties of the Paintbrush Tuff Recovered from Boreholes USW NRG-6 and USW NRG-7/7A: Data Report.* SAND95-1887. Albuquerque, New Mexico: Sandia National Laboratories. ACC: MOL.19971017.0662.

Martin, R.J., Noel, J.S., Boyd, P.J., and Price, R.H. 1997b. "Creep and Static Fatigue of Welded Tuff from Yucca Mountain, Nevada." *36th U.S. Rock Mechanics Symposium, Columbia University, New York, June 29-July 2, 1997.* p. 382. New York, New York: American Rock Mechanics Association. TIC: 250241.

Martin, R.J., Noel, J.S., Boyd, P.J., and Price, R.H. 1997c. *Creep Properties of the Paintbrush Tuff Recovered from Borehole USW NRG-7/7A: Data Report.* SAND95-1759. Albuquerque, New Mexico: Sandia National Laboratories. ACC: MOL.19971017.0661.

Martin, R.J.; Noel, J.S.; Boyd, P.J.; Riggins, M.; and Price, R.H. 1997. *Thermal Expansion of the Paintbrush Tuff Recovered from Borehole USW SD-12 at Pressures 30 MPa: Data Report.* SAND95-1904. Albuquerque, New Mexico: Sandia National Laboratories. ACC: MOL.19971017.0680.

Martin, R.J., Price, R.H., Boyd, P.J, and Haupt, R.W. 1992. *Anisotropy of the Topopah Spring Member Tuff.* SAND91-0894. Albuquerque, New Mexico: Sandia National Laboratory. ACC: NNA.19920522.0041.

Martin, R.J., Price, R.H., Boyd, P.J., and Noel, J.S. 1993a. *The Influence of Strain Rate and Sample Inhomogeneity on the Moduli and Strength of Welded Tuff.* Las Vegas, Nevada: CRWMS M&O. ACC: NNA.19930514.0013.

Martin, R.J., Price, R.H., Boyd, P.J., and Noel, J.S. 1993b. *Unconfined Compression Experiments on Topopah Spring Member Tuff at 22°C and a Strain Rate of 10^{-9} s^{-1}.* SAND92-1810. Albuquerque, NM: Sandia National Laboratory. ACC: NNA.19930728.0088.

Martin, R.J., Price, R.H., Boyd, P.J., and Noel, J.S. 1995. *Creep in Topopah Spring Member Welded Tuff.* SAND94-2585. Albuquerque, New Mexico: Sandia National Laboratories. ACC: MOL.19950502.0006.

Martin, R.J.; Price, R.H.; Boyd, P.J.; and Noel, J.S. 1994. *Bulk and Mechanical Properties of the Paintbrush Tuff Recovered from Borehole USW NRG-6: Data Report.* SAND93-4020. Albuquerque, New Mexico: Sandia National Laboratories. ACC: MOL.19940811.0001.

Martin, R.J.; Price, R.H.; Boyd, P.J.; and Noel, J.S. 1995. *Bulk and Mechanical Properties of the Paintbrush Tuff Recovered from Borehole USW NRG-7/7A: Data Report.* SAND94-1996. Albuquerque, New Mexico: Sandia National Laboratories. ACC: MOL.19950316.0087.

Nimick, F.B. 1989. *Thermal-Conductivity Data for Tuffs from the Unsaturated Zone at Yucca Mountain, Nevada.* SAND88-0624. Albuquerque, New Mexico: Sandia National Laboratories. ACC: NNA.19890515.0133.

Nimick, F.B. and Connolly, J.R. 1991. *Calculation of Heat Capacities for Tuffaceous Units from the Unsaturated Zone at Yucca Mountain, Nevada.* SAND88-3050. Albuquerque, New Mexico: Sandia National Laboratories. ACC: NNA.19910308.0017.

Nimick, F.B.; Price, R.H.; Van Buskirk, R.G.; and Goodell, J.R. 1985. *Uniaxial and Triaxial Compression Test Series on Topopah Spring Tuff from USW G-4, Yucca Mountain, Nevada.* SAND84-1101. Albuquerque, New Mexico: Sandia National Laboratories. ACC: MOL.19980602.0332.

Olsson, W.A. and Jones, A.K. 1980. *Rock Mechanics Properties of Volcanic Tuffs from the Nevada Test Site.* SAND80-1453. Albuquerque, New Mexico: Sandia National Laboratories. ACC: NNA.19870406.0497.

Papike, J.J. and Cameron, M. 1976. "Crystal Chemistry of Silicate Minerals of Geophysical Interest." *Reviews of Geophysics and Space Physics, 14,* (1), 37-80. Washington, D.C.: American Geophysical Union. TIC: 240938.

Price, R.H. 1983. *Analysis of the Rock Mechanics Properties of Volcanic Tuff Units from Yucca Mountain, Nevada Test Site.* SAND82-1315. Albuquerque, New Mexico: Sandia National Laboratories. ACC: NNA.19870406.0181.

Price, R.H. 1986. *Effects of Sample Size on the Mechanical Behavior of Topopah Spring Tuff.* *SAND85-0709.* Albuquerque, New Mexico: Sandia National Laboratories. ACC: NNA.19891106.0125.

Price, R.H. 1993. "Strength-Size-Porosity Empirical Model for Yucca Mountain Tuff." *EOS, Transactions, American Geophysical Union, 1993 Fall Meeting, October 26, 1993.* 74, 571. Washington, D.C.: American Geophysical Union. TIC: 210057.

Price, R.H. and Bauer, S.J. 1985. "Analysis of the Elastic and Strength Properties of Yucca Mountain Tuff, Nevada." *Research & Engineering Applications in Rock Masses, Proceedings of the 26th U.S. Symposium on Rock Mechanics, Rapid City, South Dakota, June 26-28, 1985.* Ashworth, E., ed. Pages 89-96. Boston, [Massachusetts]: A.A. Balkema. TIC: 218790.

Price, R.H. and Jones, A.K. 1982. *Uniaxial and Triaxial Compression Tests Series on Calico Hills Tuff.* SAND82-1314. Albuquerque, New Mexico: Sandia National Laboratories. ACC: NNA.19900810.0480.

Price, R.H. and Nimick, K.G. 1982. *Uniaxial Compression Test Series on Tram Tuff.* *SAND82-1055.* Albuquerque, New Mexico: Sandia National Laboratories. ACC: HQS.19880517.1699.

Price, R.H., Martin, R.J., Boyd, P.J., Boitnott, G.N. 1995. *Mechanical and Bulk Properties of Intact Rock Collected in the Laboratory in Support of the Yucca Mountain Site Characterization Project.* SAND94-2243C. Albuquerque, New Mexico: Sandia National Laboratories. ACC: MOL.19950130.0056.

Price, R.H., Martin, R.J., Haupt, R.W. 1994. *The Effect of Frequency on Young's Modulus and Seismic Wave Attenuation.* SAND92-0847. Albuquerque, NM: Sandia National Laboratory. ACC: NNA.19940628.0140.

Price, R.H., Connolly, J.R., and Keil, K. 1987. *Petrologic and Mechanical Properties of Outcrop Samples of the Welded, Devitrified Topopah Spring Member of the Paintbrush Tuff.* SAND86-1131. Albuquerque, New Mexico: Sandia National Laboratories. ACC: NNA.19870601.0013.

Price, R.H., Jones, A.K., and Nimick, K.G. 1982. *Uniaxial Compression Test Series on Bullfrog Tuff.* SAND82-0481. Albuquerque, New Mexico: Sandia National Laboratories. ACC: HQS.19880517.1700.

Price, R.H.; Martin, R.J., III; and Boyd, P.J. 1993. "Characterization of Porosity in Support of Mechanical Property Analysis." *High Level Radioactive Waste Management, Proceedings of the Fourth Annual International Conference, Las Vegas, Nevada, April 26-30, 1993.* 2, 1847-1853. La Grange Park, Illinois: American Nuclear Society. TIC: 208542.

Price, R.H., Nimick, F.B., Connolly, J.R., Keil, K.; Schwartz, B.M.; and Spence, S.J. 1985. *Preliminary Characterization of the Petrologic, Bulk, and Mechanical Properties of a Lithophysal Zone Within the Topopah Spring Member of the Paintbrush Tuff.* SAND84-0860. Albuquerque, New Mexico: Sandia National Laboratories. ACC: NNA.19870406.0156.

Price, R.H., Nimick, K.G., and Zirzow, J.A. 1982. *Uniaxial and Triaxial Compression Test Series on Topopah Spring Tuff.* SAND82-1723. Albuquerque, New Mexico: Sandia National Laboratories. ACC: NNA.19870406.0063.

Price, R.H., Spence, S.J., and Jones, A.K. 1984. *Uniaxial Compression Test Series on Topopah Spring Tuff from USW GU-3, Yucca Mountain, Southern Nevada.* SAND83-1646. Albuquerque, New Mexico: Sandia National Laboratories. ACC: NNA.19870406.0252.

Price, R.J., Boyd, P.J, Noel, J.S., Martin, R.J. 1994. *Relation Between Static and Dynamic Rock Properties in Welded and Nonwelded Tuff.* SAND940306C. Albuquerque, New Mexico: Sandia National Laboratories. TIC: 213482.

Thompson, A.B. and Wennemer, M. 1979. "Heat Capacities and Inversions in Tridymite, Cristobalite, and Tridymite-Cristobalite Mixed Phases." *American Mineralogist, 64*, 1018-1026. Washington, D.C.: Mineralogical Society of America. TIC: 239133.

Williams, N.H. 2001. "Contract #: DE-AC08-01NV12101 -- Thermal Test Progress Report #6." Letter from N.H. Williams (BSC) to S.P. Mellington (DOE/YMSCO), April 19, 2001, PROJ.04/01.030, with enclosure. ACC: MOL.20010612.0531.

Woodside, W. and Messmer, J.H. 1961. "Thermal Conductivity of Porous Media, I. Unconsolidated Sands." *Journal of Applied Physics, 32*, (9), 1688-1699. New York, New York: American Institute of Physics. TIC: 217510.

B.3.2   SOURCE DATA, LISTED BY DATA TRACKING NUMBER

SNF35110695001.009. Thermal and Thermomechanical Data for the Single Heater Test Final Report. Submittal date: 08/24/1998.